Superconductivity: The Path of Least Resistance to the Future

William J. Mercer and Yuri A. Pashkin

Department of Physics, Lancaster University, Lancaster LA1 4YB, United Kingdom

ARTICLE HISTORY
Compiled June 19, 2023

ABSTRACT
The accidental discovery of mercury's zero resistance at temperatures lower than 4.2 K which took place in 1911 by the Dutch physicist Heike Kamerlingh Onnes in his laboratory at the University of Leiden, appeared to be one of the greatest breakthroughs of physics of all time. It has led to the creation of an entirely new field within physics called superconductivity; this attracted many of the finest minds in physics whose work in this area produced no less than six Nobel Prizes to date. Zero resistance, together with the expulsion of magnetic fields which was discovered many years later, are the two unique and intriguing properties of superconductors which puzzled scientists' brains for a proper theoretical explanation of the observed phenomena. However in 1935, the phenomenological theory proposed by Fritz and Heinz London (known as the London theory) was the first success in the field, which was followed in the 1950s by another phenomenological theory put forward by Vitaly Ginzburg and Lev Landau. Despite this, a satisfactory microscopic theory for superconductivity had to wait until 1957 when John Bardeen, Leon Cooper and John Robert Schrieffer proposed their theory, whic was nicknamed the BCS theory in their honour. The more recent discovery of the cuprate high temperature superconductors (HTS) in 1986 gave a new momentum to the field and intensified the search for room temperature superconductors which continues to this day. While this quest is under way, and new theories of superconductivity are being developed, physicists, material scientists and engineers are using superconductors to establish new technologies and build machines, devices and tools with unprecedented properties. Today superconductors are widely used in healthcare, particle accelerators, ultrasensitive instrumentation and microwave engineering and they are being developed for use in many other areas as well. In this review, we will trace the history of superconductors and provide a brief overview into some of the recent applications of superconductivity.

KEYWORDS
zero electrical resistance; Meissner effect; flux quantisation; London theory; Ginzburg-Landau theory; BCS theory; Josephson effect; high-temperature superconductivity; superconductive electronics; SQUID; superconducting qubit

PACS CLASSIFICATION

1. Introduction

Superconductivity is usually defined as 'the complete disappearance of electrical resistance in various solids when they are cooled below a characteristic temperature' [1]

CONTACT Yuri A. Pashkin Email: y.pashkin@lancaster.ac.uk

(also described as $0\,\Omega$, where Ω is a capital Greek letter omega commonly used to denote the unit of resistance in the SI system, the Ohm). The characteristic temperature to observe this phenomenon is often below 10 K. Because of this, superconductivity falls under the broader field of research known as low temperature physics. Discovered in mercury over 100 years ago, this phenomenon remained a puzzle to scientists for several decades after its discovery which meant that new insights in physics were needed for its understanding. Over this whole period, many scientists have contributed to superconductivity research making the field a truly global collaborative effort and in the process providing much needed knowledge which has had a strong impact on many other fields. Ever since the discovery of superconductivity, many in the scientific community have been inspired by the multiplicity of its possible applications and its potential to create new technologies, or significantly improve existing ones. The major hurdles encountered to these developments were the low temperatures required to bring materials to below their critical temperature. For example, the highest critical temperature of an elemental superconductor, niobium, is 9.2 K, just a factor of two higher than the temperature of liquid helium, but despite this constraint, scientists and engineers have already been able to develop a wide variety of applications of superconductors (such as superconducting solenoids in MRI scanners or extremely sensitive magnetometers to measure weak magnetic signals produced by the human brain and to study magnetic properties of solids).

Cryogenics (engineering techniques and machines used to reach very low temperatures) have recently become helium free, which means that no liquid helium bath is needed now to maintain low temperatures required for superconductivity. As the price of liquid helium rises this development has significantly reduced cooling costs. Moreover, refrigerators used in the experimental laboratories have become more accessible and user-friendly; and this has been of great assistance in the development of superconductivity applications. Even more encouraging is the recent hope that superconductivity will be observed in a material at room temperature which would of course mean that superconductivity could be much more widely used. For example, the use of superconducting wires and cables in the electrical power and transmission grids would result in enormous energy savings. Moreover, if cryogenics were no longer required for superconductivity, many more applications of it would become more compact and cheaper. This is why there is a worldwide concerted effort by industrial laboratories, national research institutes and universities at present to synthesise a material which will be a superconductor at room temperature.

In looking back at the progress of research into superconductivity, it is possible to see science and technology working hand in hand for mutual benefit, where technology drove science, which in turn drove technology. The initial discovery of superconductivity was only made possible by the technology of cryogenics; Heike Kamerlingh Onnes had built a unique liquefier capable of reaching temperatures of approximately 4 K. By reducing the pressure of the liquid helium, the temperature was lowered still further to near 1.5 K. In 1911, these were the lowest temperatures ever recorded on Earth, and this led directly to the discovery of superconductivity. Following this, multiple novel technologies were developed utilising superconductivity, which will be reviewed later in this paper. And from superconductivity came the prediction and observation of the Josephson effect (reference needed), which gave rise to the entirely new field of superconductive electronics.

This review is organised as follows. Firstly, we give a brief historical overview of superconductivity research, highlighting major breakthroughs in the field. We then turn to the applications of superconductors, superconducting devices and tools. The

applications are divided into two groups: large-scale applications and electronic applications. The first group is based on using bulk superconductors in the form of wires and cables used on their own or wound into coils or solenoids, or large pieces of superconductors shaped into wheels, cavities, etc. Electronic application usually require deposition and patterning of thin superconducting films and creation of multi-layer structures. This is done using various well-developed lithographic techniques which control the feature size down to about 10 nm. Finally, we summarise the report.

2. Key milestones in the superconductivity research

2.1. The discovery of superconductivity

Here we highlight the major milestones in the superconductivity research. For a more detailed history please consult Steven Blundell's book [2]. More information may be found in several books and journal publications released to celebrate the 100th anniversary of the discovery of superconductivity in 2011 [4–7].

The discoverer of superconductivity, Heike Kamerlingh Onnes was the Physics Chair at the Physical Laboratory at the University of Leiden from 1882 to 1923. His research was mainly focused on Low Temperature Physics, with his first major technological breakthrough occuring in 1908 when he was able to liquefy helium. Hence he possessed the best cryogenic machinery at the time and this was a crucial factor in the discovery of superconductivity. His main rival in the field of cryogenics was Sir James Dewar, a British chemist and physicist who is famous for the invention of a special vacuum flask for storing cryogenic liquids, had succeeded in liquefying hydrogen in 1898, eight years before Kamerlingh Onnes, but fell behind in liquefying helium. The liquefaction of helium was the experimental confirmation of the theory of Johannes van der Waals, a professor at the University of Amsterdam, according to which all the gases should become liquids at sufficiently low temperatures. At that time scientists were not aware that there are two isotopes of helium: He4 with two protons and two neutrons and He3 with two protons and one neutron, and only He4 was liquefied. The abundance of He3 is much smaller than that of He4, hence this was only discovered in 1939.

Kamerlingh Onnes was experimenting with a platinum wire and found that its resistance did not change below 4.2 K. From this result, he concluded that the resistivity of the sample had fallen to a minimum value which depended on the sample's purity. This was in agreement with the earlier results obtained by Dewar who was measuring resistivity of gold and silver samples and observed its saturation at 16 K. This called for samples of higher purity and so Kamerlingh Onnes chose to focus on mercury which could be purified to a higher degree as compared to other metals. Mercury is a liquid at room temperature, but solidifies at about -39°C. Hence, it was possible to make wires by filling very fine glass capillaries with mercury and cooling them down. For resistance measurements, metal electrodes were attached at both ends.

During one of the experiments conducted in April 1911, while the mercury sample was cooled below 4.2 K, its resistance suddenly dropped to zero. Kamerlingh Onnes and his team first attributed this to a short circuit in the experimental apparatus and ran the experient again. However the same behaviour was observed in repeated experients consistently. However, upon raising the temperature of the mercury above 4.2 K the electrical resistance suddenly re-emerged. From this, Kamerlingh Onnes realised that the zero resistance was not an experimental artefact, but a new state of matter which sets in below a certain temperature. This is the first recorded measurement of

the phenomenon initially referred to as supraconductivity known today as superconductivity and is shown in Fig. 1. The temperature below which a material becomes superconducting is known as the critical temperature and is commonly denoted as T_c.

Among the elements of the periodic table, 31 are superconductors at ambient pressure. At higher pressure, the number of elemental superconductors exceeds 50.

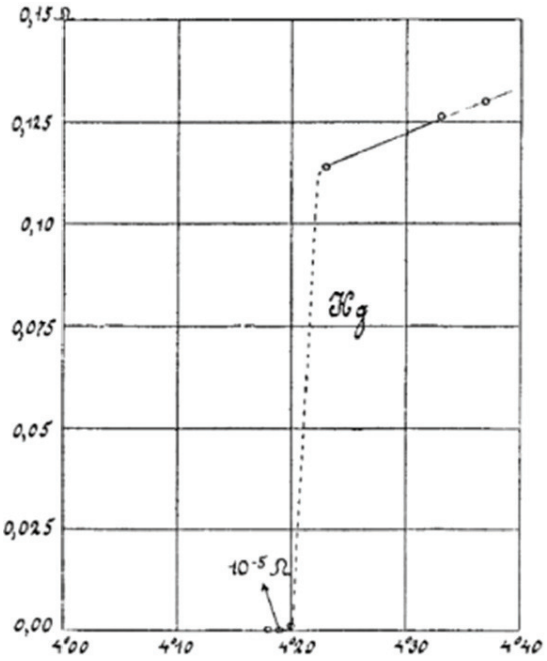

Figure 1. The graph from Kamerlingh Onnes' notes which shows the change in resistivity of mercury as temperature changes. From Ref. [3] with permission.

The main drive for doing resistivity measurements at low temperatures was to test three major theories existed at the time that predicted the behaviour of the resistance of a material at temperatures close to the absolute zero, see Fig 2 [2]. The famous Sir William Thomson later known as Lord Kelvin, the British scientist after whom the Kelvin scale is named, believed that electrons were bound to their respective atoms and therefore the resistivity would tend to go to infinity as temperatures reached closer towards absolute zero. An earlier theory existing at the time by Augustus Matthiessen, another British chemist and physicist, stated that the resistivity would fall to a constant non-zero value. Dewar was convinced that the resistance would go to zero as the temperature fell. Heike Kamerlingh Onnes' results on non-superconducting metals confirmed the theory of Matthiessen, however, none of the three theories were able to predict the abrupt change in resistivity [4,7].

Upon publication of Kamerlingh Onnes's results, many scientists started to consider the potential applications of this new phenomenon. H. Kamerlingh Onnes himself suggested that it would be possible to create very strong magnetic fields using a superconducting wire. 'The solution of the problem of obtaining a field of 100,000 G could be obtained by a coil of say 30 cm in diameter and the cooling with a plant which could be realized in Leiden with a relatively modest financial support' [8]. However, in a further experiment in January 1914, he discovered that at a temperature of 4 K the superconducting properties of lead were destroyed by an external magnetic field of only 600 G (the effect presently known as quenching) [9]. This critical magnetic field H_c constraint was a severe limitation upon contemporary ambitions to produce supercon-

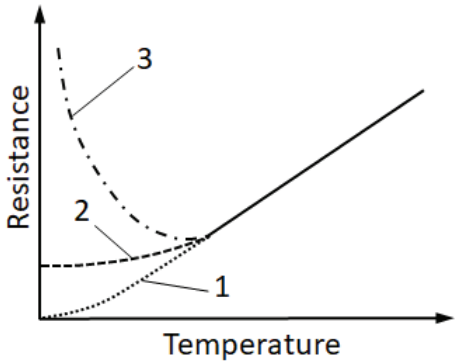

Figure 2. Different predictions for temperature dependence of electrical resistance.
1. The resistance approaches a zero value with decreasing temperature (Sir James Dewar, 1904);
2. The resistance approaches a finite limiting value (Augustus Matthiessen, 1864);
3. The resistance could pass through a minimum and approach infinity at very low temperatures (Sir William Thomson (Lord Kelvin), 1902)

.

ducting magnets and was overcome only after the discovery of type II superconductors in the 1950s.

Interestingly, the discovery of superconductivity by Kamerlingh Onnes was not fully recognised by his contemporary scientists. This is clear from the wording of the Nobel Prize in Physics which he was awarded in 1913 for (in the words of the committee) "his investigations on the properties of matter at low temperatures which led, inter alia, to the production of liquid helium".

2.2. The Meissner-Ochsenfeld Effect

Another notable physicist within the field of superconductors was Walther Meissner, a German low temperature physicist of the early 20th century. By 1927 he had established a laboratory capable of reaching superconducting temperatures at the Imperial Physical Technical Institute (PTR) in Berlin. In this laboratory, Meissner was able to discover a number of new superconductors including tantalum (Ta, $T_c = 4.4\,\mathrm{K}$), thorium (Th, $T_c = 1.4\,\mathrm{K}$) and niobium (Nb) which had the highest critical temperature $9.2\,\mathrm{K}$ among the elemental superconductors [10]. However, Walther Meissner's most notable contribution to the field is the paper he published in 1931 in collaboration with a fellow German physicist working at PTR called Robert Ochsenfeld. In their joint paper 'A new effect concerning the onset of superconductivity', they outlined their experiments into the quenching effect of a magnetic field on superconductivity [11]. During their experimentation on pure tin and lead, they found that when the metals reached their transition temperature, magnetic flux was expelled from the interior of the superconductor and magnetic induction vanished (see figure 3). Furthermore, when the magnetic flux was increased above the critical magnetic field H_c, the flux completely penetrated the material causing superconductivity to be quenched, but upon lowering the field below H_c the flux was again expelled and superconductivity was restored. The expulsion of the magnetic field from the superconductor was named the Meissner-Ochsenfeld effect in their honour. This behaviour showed that a superconductor not only has zero resistivity, but that it also expels the magnetic field from within. According to Maxwell's equations (specifically the Ampere-Maxwell law), it

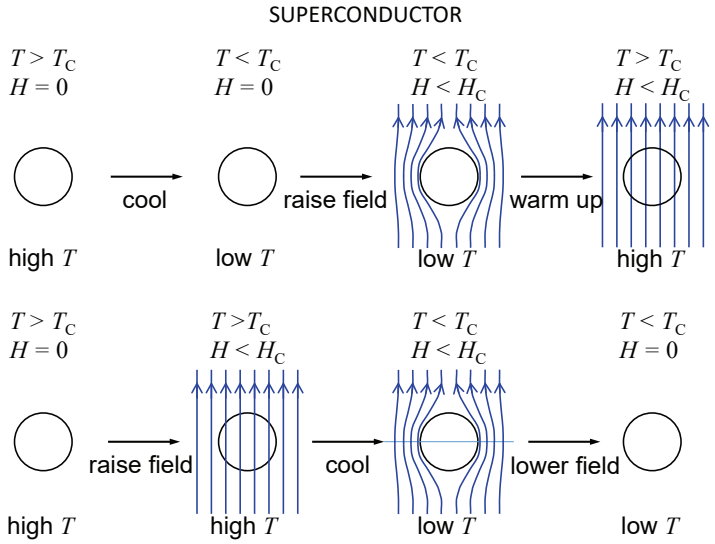

Figure 3. Behaviour of a superconductor in a magnetic field when cooled below the transition temperature in two different ways. (Upper) Cooling of a superconductor below T_c in zero magnetic field. (Lower) Cooling of a superconductor below T_c in weak magnetic field (lower than H_c) results in the expulsion of the field from the superconductor (Meissner-Ochsenfeld effect).

was expected that an ideal conductor would have zero resistance and it would trap magnetic flux inside. However, the discovery of the Meissner-Ochsenfeld effect challenged the assumption that a superconductor is an ideal conductor and instead proved that superconductivity occurs due to a thermodynamic equilibrium.

2.3. London theory

Further theoretical work was developed on the Meissner-Ochsenfeld effect by brothers Fritz and Heinz London in Oxford in 1935. London theory (named after its creators) is a phenomenological theory aiming to explain the Meissner-Ochsenfeld effect rather than explaining the exact nature of superconductivity. Using Maxwell's equations, they produced the equations which describe the magnetic and electric fields within a superconductor:

$$\mathbf{E} = -\frac{1}{c}\frac{\partial \mathbf{A}}{\partial t} - \nabla\phi, \tag{1}$$

$$\operatorname{curl}\mathbf{H} = \frac{4\pi\mathbf{j}}{c}, \tag{2}$$

where $\mathbf{E}$ is the electric field, $\mathbf{A}$ is the vector potential, c is the speed of light in a vacuum, t is time, ϕ is the scalar potential, $\mathbf{H}$ is the magnetic field density and $\mathbf{j}$ is the electric current density. They then go on to prove that the solution to this should be solved by:

$$\mathbf{E} = \frac{4\pi\lambda_L^2}{c^2}\frac{\partial \mathbf{j}}{\partial t} \tag{3}$$

where m is the mass of an electron, n_s is the number density of electrons and e is the charge of an electron. It was found that the electric field within a superconductor due to an external magnetic field drops off exponentially quickly. This exponential drop-off occurs within a small layer very close to the surface of the material. Further into the material, the magnetic field in the superconductor is effectively zero and has been expelled. It was realized that the currents running through the boundary layer create magnetic fields which cancel out the external magnetic field, thus creating a net zero field internally [12]. London theory provides a good agreement with many real superconductors provided the temperature is not too low. In these circumstances, London theory breaks down as it fails to account for the quantum behaviour of electrons at these low temperatures [13].

2.4. Early experimental progress in superconductors

In conjunction to the work being done on pure metal superconductors, experiments were also being conducted to find different types of superconducting materials. This work started with the experiment in 1929 by Wander Johannes de Haas and Willem Hendrik Keesom, who were working in the Kamerlingh Onnes Laboratory at the University of Leiden, in which they created an alloy (4% bismuth into gold) and found that Au_2Bi became a superconductor below 1.9 K. This discovery was particularly interesting as neither pure metal exhibited superconductivity at ambient pressure [14].

The next step in this area of research was the later report on the experiments of de Haas and Casimir-Jonker (another physicist at Leiden) in 1934 [15]. In their report they outlined their experiments with lead-thallium (Pb+64.8wt%Tl) and bismuth-thallium (Bi+37.5at.%Tl) alloys. In their experiments, they carefully prepared a cylindrical sample of the superconducting alloy and applied a magnetic field perpendicular to the axis of the cylinder. The magnetic field was measured on the inside of the cylinder and as the magnetic field was increased it was found that the magnetic field began to penetrate the superconductor in the outer region, but not the inner region. It was discovered that an increasing magnetic field gradually penetrated the superconductor, unlike in pure metals where an external magnetic field above the critical field H_c would completely and instantaneously penetrate the superconductor (Meissner-Ochsenfeld effect) [15].

In 1931, a scientist called Lev Shubnikov (who had previously worked with Wander de Haas at the Kamerlingh Onnes Laboratory) became the head of the Cryogenics Laboratory in the Ukrainian Physical-Technical Institute (UPhTI) founded in the USSR in 1928 and decided to go into superconducting alloys research. He submitted a paper alongside Rjabinin (another physicist working at UPhTl) in which they outlined their support for the existence of a gradual penetrating magnetic field that they termed H_{c1} after their research with different lead-thallium alloys (Pb+66.7at.%Tl) and a lead-bismuth alloy (Pb-35wt%Bi). They also experimented with increasing the magnetic field past H_{c1} to a magnetic field strength which destroyed the superconductivity in the alloy (a field strength they termed H_{c2}) [16]. Their results suggested that superconductivity in alloys may be different than superconductivity in pure metals.

A few months later in April 1935, scientists Kurt Mendelssohn and J.R. Moore working at the University of Oxford submitted their experiment on a lead-bismuth alloy (Pb+70wt%Bi) in which they also supported the existence of a gradual penetrating magnetic field [17]. They, however, proposed the 'Mendelssohn Sponge' hypothesis which suggested that the inhomogeneities in the structure of superconducting alloys

caused the superconductor to have a network of thin superconducting threads (with a sponge-like structure) so that in some parts of the superconductor the superconductivity is quenched by the magnetic field, while in other parts superconductivity still remains with zero flux [18].

In 1936 and 1937 a number of very important papers on superconductivity were published by Shubnikov and colleagues at UPhTl outlining a number of key experiments in the field of superconducting alloys. Using the alloys Pb-Tl (0.8; 2.5; 5; 15; 30; 50wt.%) and Pb-In (2; 8wt.%) they conducted a number of experiments and came to the following conclusions:

1. Pure superconductors exhibited the Meissner-Ochsenfeld effect in which a magnetic field H_c completely penetrated the superconductor whereas in a superconducting alloy the material expelled any internal magnetic field up to H_{c1}. After this value, the material remained superconducting, but the magnetic field began to penetrate into the material. When H_{c2} was reached the material stopped being superconductive (see Fig. 4).
2. Increasing the impurity concentration decreased the value of H_{c1} and increased the value of H_{c2}.
3. The superconductors selected were homogenous and were all of a single phase. This ruled out the Mendelssohn Sponge hypothesis [19] being responsible for the superconducting properties (this was confirmed using X-ray analysis of the materials).

These conclusions effectively ruled out the Mendelssohn Sponge hypothesis and laid the foundations for a new classification of superconductors referred to as Type II superconductors today. These findings had major implications on understanding of the behaviour of superconductors in external magnetic fields and facilitated development of strong magnets using solenoids made of Type II superconductors. Despite this ground-breaking work, the Mendelssohn Sponge hypothesis was the dominant theory in superconducting alloys for around 25 years. This can largely be attributed to the political circumstances at the time when tragically Lev Shubnikov was arrested and executed in 1937 as part of Stalin's purges. A theory describing the formation of the so-called Shubnikov phase, between H_{c1} and H_{c2}, was developed 20 years later.

2.5. The foundations of modern superconductivity theory

After this setback, it was only after the Second World War, that significant progress began to be made in the field of superconductors when Vitaly Ginzburg and Lev Landau (theoretical physicists in the USSR) published their paper on the Ginzburg-Landau Theory (GL theory) [20,21]. GL theory was introduced with the aim to improve London theory by considering how superconductivity can be destroyed by a critical current Jc running through the superconductor. A key aspect of the GL theory was the addition of an order parameter ψ, such that $\psi = 0$ above T_c and $\psi \neq 0$ below T_c. The order parameter has the following relation to the number density of electron pairs n_s:

$$n_s = |\psi|^2. \tag{4}$$

The difference in free energy, F, of the material between the superconducting and nonsuperconducting states is then calculated by using a second order approximation

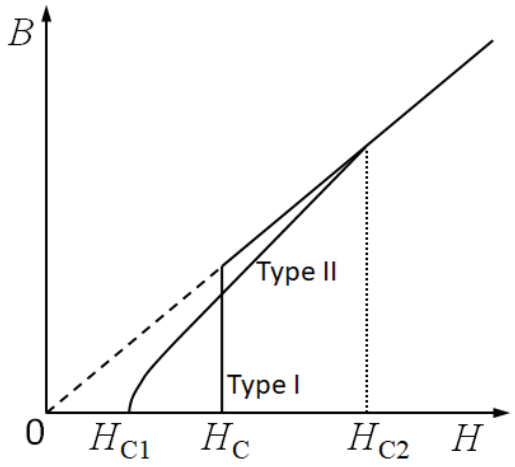

Figure 4. A graph showing the dependence of magnetic flux density B of each type of superconductor on an external magnetic field H.

.

(which is valid when T is near T_c). This free energy difference is the following:

$$\delta F_{\mathrm{sn}} = F_{\mathrm{s}} - F_{\mathrm{n}} = \alpha|\psi|^2 + \frac{\beta}{2}|\psi|^4 + \frac{1}{2m}\left|\psi\left(i\hbar\nabla + \frac{2e}{c}\right)\right|^2 + \frac{H^2}{8\pi}, \tag{5}$$

where α and β are constants and $\hbar$ is the reduced Planck's constant and m is the electron mass. The minimisation of this function gives the solutions for the wavefunction. This gives two characteristic parameters, the coherence length, $\xi(T)$, which describes the variation of the wavefunction in space and the penetration depth, $\lambda(T)$, which is equivalent to the London penetration depth:

$$\xi(T)^2 = \frac{\hbar^2}{4m|\alpha|}, \tag{6}$$

$$\lambda(T)^2 = \frac{mc^2}{4\pi n_s e^2}. \tag{7}$$

These two parameters can be combined into the GL parameter κ, independent of temperature and is a characteristic of a given material [21,22]

$$\kappa = \frac{\lambda(T)}{\xi(T)} = \frac{mc}{\hbar e}\sqrt{\frac{\beta}{2\pi}}. \tag{8}$$

It can be shown that $\kappa \ll 1$ in the pure superconductors and $\kappa \gg 1$ in the dirty or in the high-temperature superconductors. The value $\kappa = 1$ separates superconductors of type I and II.

In May 1950, theoretical physicist Herbert Fröhlich (who was working in the University of Liverpool at the time) outlined his theory on superconductivity which suggested that electron-lattice interactions are key to understanding superconductivity

Table 1. Average mass of each isotope of mercury and its corresponding critical temperature T_c. This table is reproduced from ref. [23].

Isotope	Average mass	T_c (K)
1	203.4	4.126
2	202.0	4.143
3	200.7	4.150
4	199.7	4.161

(through the interactions between electrons and lattice vibrational quanta often called phonons) [25]. It followed from his theory that both T_c and H_c should be proportional to $M^{-1/2}$, where M is the nuclear mass, for isotopes of the same element. The experiments confirming this isotope effect were carried out earlier that year by two groups independently and without knowledge of each other's work. The two groups, one at the National Bureau of Standards and the other at Rutgers University in the US, measured critical temperatures of different isotopes of mercury [23,24]. Both groups found that different isotopes tested produced different critical temperatures (see Table 1). These important experiments contributed greatly to the understanding of superconductivity and to the development of a microscopic theory of it a few years later.

In 1956 Leon Cooper (a physicist working in the University of Illinois) built on Fröhlich's work by laying out the concept of Cooper pairs in superconductors in his paper [26]. This work was then expanded by John Bardeen (the only person to ever be awarded two Nobel Prizes in Physics) and Robert Schrieffer (both were physicists at the University of Illinois) in subsequent papers to give a complete microscopic theory of superconductivity which was coined the Bardeen-Cooper-Schrieffer theory (BCS theory) [27]. They were jointly awarded the Nobel Prize in Physics in recognition for their efforts in 1972.

2.6. An overall description of BCS theory

To understand BCS theory, a little background information about materials is first necessary. In a metal, positively charged ions (arranged in a lattice) are surrounded by a 'sea' of delocalised free electrons. As these electrons are delocalised (not associated with any one ion), they are free to move between the ions and carry charge and spin [28]. Importantly, electrons obey the Fermi-Dirac statistics which describes how quantum states at different energies are occupied. According to the Pauli exclusion principle, no more than one electron can occupy a quantum state. There exists another class of particles called bosons, to which the Pauli exclusion principle does not apply. This makes the properties of bosonic systems completely different from those of fermionic systems, in particular, condensation becomes possible when a large number of bosons occupy the same quantum state with the lowest energy.

In BCS theory we picture what happens if there is a single negatively charged electron in between a lattice of positively charged ions. As they are oppositely charged there will be an attractive force between the electron and the ions. The electron pulls all the surrounding ions closer to itself, distorting the ionic lattice around the electron. As the positive ions have all been pulled closer together the region surrounding the area looks like a positively charged cloud. This positively charged cloud attracts another electron with an opposite spin and so the electrons have effectively been linked forming a Cooper pair with zero total spin, i.e., a bosonic particle. The distance between the

two electrons in a Cooper pair (termed the coherence length and can be from tens of nanometres to microns in a conventional superconductor) is usually much larger than the scale of the lattice (0.5–1 nm) in a conventional superconductor. This large coherence length subtly implies that there can be many Cooper pairs within a given volume that overlap. This way the so-called superconducting condensate is formed in which all Cooper pairs have exactly same energy. Hence the whole condensate of Cooper pairs in a block of a superconductor, no matter how big it is, is described by the wavefunction ψ, called the order parameter in GL theory, see Section 2.5.

The main parameter of the BCS theory is the superconducting energy gap, usually denoted as Δ, which is a material parameter. The gap is the binding energy of two electrons in every Cooper pair forming the condensate. It is maximal at zero temperature and is related to the critical temperature of a superconductor as $\Delta(0) \simeq 1.76\, k_{\mathrm{B}} T_{\mathrm{c}}$, where k_{B} is the Boltzmann constant. The gap is a monotonically decreasing function of T: it is almost constant at $T \ll T_{\mathrm{c}}$, but around T_{c} goes to zero as $\Delta(T) \simeq \Delta(0)\left(1 - \dfrac{T}{T_{\mathrm{c}}}\right)^{1/2}$. The presence of energy gap explains some features observed in electron transport through tunnel junctions (see Section 2.8) and in the interaction of superconductors with electromagnetic radiation (see Section 5.3).

2.7. The unification of BCS and GL theory

An important development in the field of superconductivity was when Alexei Abrikosov (a physicist working in the USSR and a former student of Landau) wrote a paper in 1957 [29] which considered what happened when the Ginzburg-Landau parameter becomes larger than $\dfrac{1}{\sqrt{2}}$. This idea was initially overlooked by Ginzburg and Landau and they strongly discouraged Abrikosov from publishing for many years. In his paper, Abrikosov compared his theory with the experiments done by Shubnikov and was finally able to discredit the Mendelssohn sponge theory and distinguish between type I and type II superconductors [29,30]. For their contribution to the theory of superconductivity, both Ginzburg and Abrikosov were awarded the Nobel Prize for Physics in 2003.

In 1959 the macroscopic GL theory and the microscopic BCS theory were finally combined by Lev Gor'kov (a physicist in the USSR) who was able to show that GL theory was a limiting form of BCS theory at $T \to T_c$. A particularly interesting result from Gor'kov's work, was that he was able to characterise the Ginzburg-Landau parameter in terms of the size of a Cooper pair and the London penetration depth. This proof enabled widespread acceptance and usage of GL theory [31]. Both BCS and GL theory now form the basis of our understanding for superconductivity and are in widespread use.

2.8. The Josephson effect

The concept of a Josephson junction was first theorised by Brian Josephson in 1962 who at that time was a PhD student at the University of Cambridge [32]. In its simplest form, a Josephson junction is simply two superconducting electrodes separated by a thin layer of insulating material (see Fig. 5(a)). The insulating layer presents a barrier for Cooper pairs through which, according to classical physics, they cannot penetrate, however, in quantum mechanics by the process known as tunnelling, the

Cooper pairs can pass through. Under BCS theory, a Cooper pair condensate consisting of a large number of Cooper pairs is described by a single wavefunction associated with the density of Cooper pairs in a bulk superconductor. Due to their quantum nature, the wavefunctions of the two condensates 'leak' into the insulating layer from both sides. This means it is possible for the wavefunctions to penetrate far enough into the material that the wavefunctions overlap (see Fig. 5(a)). This overlap means that Cooper pairs are able to travel through the insulating material without experiencing any resistance. Nonetheless the presence of the insulating layer in between the two superconductors limits the magnitude of current that can pass through the junction, creating a critical current of the junction that is much smaller than the critical current of the two superconducting electrodes (see Fig. 5(b)). The critical current of this junction is controlled by choice of material, size of the junction, thickness of the insulating layer and the temperature. This effect, referred to as the DC Josephson effect, was first observed by Phillip Anderson and John Rowell in 1963 [33] and can be described by the following equation:

$$I = I_c \sin \phi, \tag{9}$$

where I is the current flowing through the junction, I_c is the critical current of the junction and ϕ is the phase difference between the superconducting electrodes. Hence one can control the phase difference by DC current.

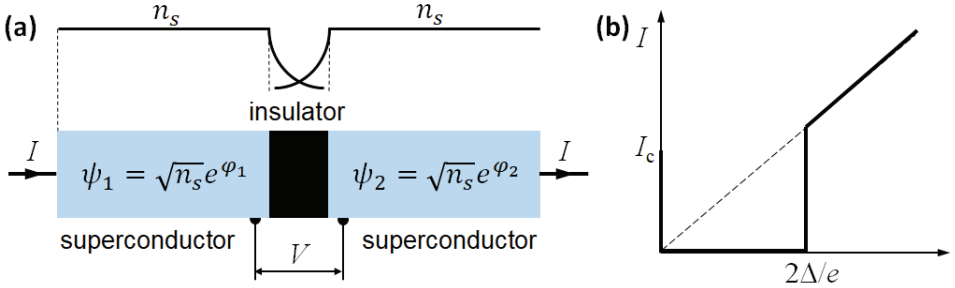

Figure 5. (a) Schematic of a Josephson junction. A thin layer of insulator is placed in between two superconducting materials. For simplicity, the two electrodes are made of the same superconductor with Cooper pair number density n_s. The wavefunctions in the left and right electrodes have a phase difference $\phi = \phi_1 - \phi_2$ controlled by the external current I (see Eq.(9)). (b) Schematic of the current-voltage characteristic of a Josephson junction consisting of the supercurrent branch up to I_c and the quasiparticle branch at voltages above $2\Delta/e$.

Once the DC current exceeds I_c, the junction becomes resistive and the voltage drops across it (Fig. 5(b)). In this case the phase difference starts to oscillate in time according to

$$\frac{d\phi}{dt} = 2eV/\hbar, \tag{10}$$

where V is the voltage drop across the junction, e is the electron charge and $\hbar$ is the reduced Planck's constant. Equation (10) describes the AC Josephson effect, which underpins the voltage standard based on the Josephson effect (see Section 5.2). However, the most common application of Josephson junctions is in superconducting quantum interference devices (SQUIDs) which are extremely sensitive magnetometers (see

Section 5.1). For the prediction of the effect named after him, Brian Josephson was awarded the Nobel Prize in Physics in 1973.

2.9. A breakthrough in high Tc superconductors

By the early 1980s a large amount of research had been conducted into intermetallic structures with the aim of increasing the temperature at which superconductivity occurs, unfortunately this yielded disappointing results, (for example the highest T_c achieved by 1985 was 23.3 K). Scientists' aim at the time was to produce materials which had a critical temperature above the boiling point of liquid nitrogen (77.4 K) [34]. Superconductivity above this temperature would enable more widespread use of superconductors as liquid nitrogen cooling is significantly cheaper than liquid helium cooling. Superconductors with a critical temperature above 77.4 K are commonly known as high-temperature superconductors (HTS) and represent the most active area of materials research at this present time [35].

In 1985, scientists Georg Bednorz and Alex Müller were working on high-temperature superconductivity in the IBM Zürich Research Laboratory in Switzerland. They decided that 'no further progress could be achieved with intermetallic compounds' [36] and so they started to experiment with metallic oxides with the hopes of achieving a high T_c. Their experiments were based on the idea of creating Jahn-Teller polarons which would indicate a strong interaction between the electrons and distortions in the lattice enabling superconductivity at higher temperatures [37]. At first they experimented with nickel oxide compounds but they failed to find high critical temperatures. After a lack of progress, they then turned to copper oxide compounds and in 1986 in their experiments with Ba-La-Cu-O systems they were able to achieve a critical temperature of $T_c \approx 30$ K [38]. Within a very short period of time after publication, a number of new materials were found with a high critical temperature. By 1987 physicists Paul Chu and Maw-Kuen Wu working in the University of Houston and the University of Alabama, respectively, achieved a critical temperature of 93 K, the first material discovered to be classed as a high temperature superconductor [39] (see Fig. 6). Bednorz and Müller revolutionized the field of superconductors with the discovery of the copper oxide superconductors (commonly known as the cuprates). Their CuO_2 superconducting layers separated by insulating layers is the only family of superconductors with critical temperatures higher than 77.4 K [36]. Although there is still disagreement up to now on the exact mechanism responsible for superconductivity in the cuprates, Bednorz and Müller were awarded a joint Nobel Prize in Physics in 1987 (the fastest recognition of research in the history of the Nobel Prize in Physics).

Since this big step-like increase in the critical temperature of superconductors, further progress in this research area was rather modest. In 2001, superconductivity in MgB_2 was discovered with a critical temperature of 39 K [41], which was the highest transition temperature measured by that time for a non-copper-oxide bulk superconductor. In terms of its composition, MgB_2 differs strikingly from most low-temperature superconductors, however, its superconducting mechanism is primarily described by BCS theory. In 2006, a novel class of superconducting materials, called pnictides, was discovered [42]. This class is based on conducting layers of iron and a pnictides (chemical elements in group 15 of the periodic table, typically arsenic (As) and phosphorus (P)), unlike the high-temperature superconductors which are based on layers of copper and oxygen sandwiched between other substances (La, Ba, Hg). While the critical

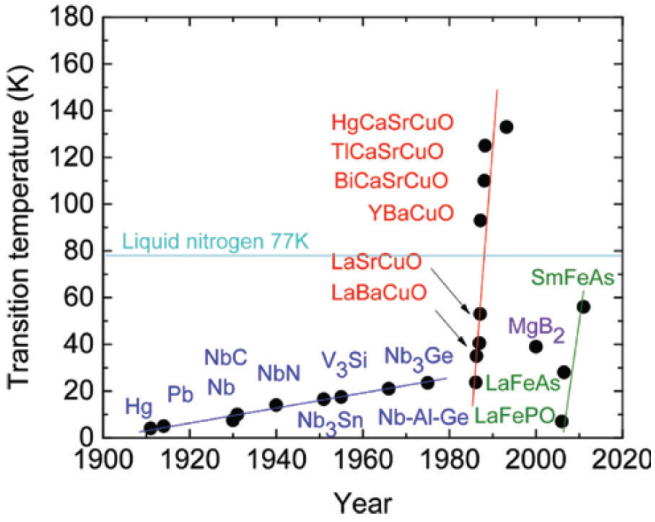

Figure 6. Timeline of the discoveries of various families of superconductors. A big jump occurred in 1986 when the so-called high-temperature superconductors were discovered allowing the use of superconductors at temperatures above the boiling temperature of liquid nitrogen. From Ref. [40] with permission.

.

temperature of iron-based pnictide superconductors is typically in the range 10–60 K, these new compounds are very different from the cuprates and may help lead to a theory of non-BCS-theory of superconductivity.

3. Applications

3.1. The first practical application of superconductivity

Since the discovery of superconductivity scientists and engineers have thought about potential applications of such an interesting phenomenon. There are a vast array of potential applications of superconductors across a huge number of fields. However, to date, the actual practical applications of superconductors have been very limited. In 1954 the first application of superconductivity was by George Yntema (working at the University of Illinois). Yntema constructed the first superconducting magnet using niobium wire. He chose niobium after finding a critical field plot, only later discovering that superconducting magnets were supposedly unfeasible in niobium according to the Mendelssohn Sponge model. Despite this, he was able to produce a field of 0.7 T at 4.2 K [43].

3.2. A variety of applications for superconductors

Since Yntema's work in 1954, a number of applications of superconductors have developed. Their practical uses remained relatively limited for some time due to the very low temperatures needed for superconductivity to occur (which meant the use of very expensive helium cooling). However, after the discovery of cuprate high-temperature superconductors it became viable to use superconductors in a wider variety of applications. The list below presents the current applications of superconductors. However, it is highly probable, that as the properties of available superconductors improve, the

number of applications will significantly increase.

Fundamental research: quantum computing, quantum sensing, physics of artificial atoms, on-chip quantum electrodynamics, single microwave photon generation and detection, search for dark matter using ultralow-noise amplifiers.

Electronics: ultrasensitive magnetometry, various types of detectors for astronomy, voltage standards, digital circuits.

Microwave components: high-quality-factor resonators, filters, delay lines, antennae.

Medical techniques: SQUID-based magnetoencephalography (MEG) and electrocardiography (ECG), magnetic resonance imaging (MRI).

Large scale applications: cables, switches, current limiters, generators, motors, transformers, fusion, MAGLEV trains.

3.3. Selecting the appropriate superconductor for the application

When choosing a superconductor, a number of material properties are key:

1. Critical temperature T_c – A high critical temperature may mean that less energy is used cooling the superconductor to below the transition temperature.
2. Critical current density J_c – The maximum current density that a superconductor can carry before losing its superconducting properties.
3. Critical magnetic field H_c – In type II superconductors the important parameter is H_{c2}. This is the maximum external magnetic field that can be applied before the material is no longer superconducting.
4. Quality of Josephson junctions fabricated from superconducting materials. This is critical for electronic applications in which the Josephson junction plays key role.

Cuprate high-temperature superconductors (HTS) typically outperform other superconductors in critical temperature, critical current density and critical magnetic field, making the cuprates a very attractive choice for practical applications. There are a few drawbacks to using cuprate HTS which mostly arise due to the layered nature of the material that makes it more difficult to work with than other materials and needs to be taken into consideration when designing applications. The major drawback of HTS is that there is no fabrication recipe for producing high-quality Josephson junctions, hence electronic applications are dominated by conventional superconductors.

4. Large scale applications

4.1. Magnetic Resonance Imaging

By far the most common use of superconductors today is in Magnetic Resonance Imaging machines (commonly known as MRI scanners). It is estimated that there are over 10,000 globally installed MRI machines with superconducting magnets [44]. An MRI machine provides a noninvasive method of identifying a wide variety of medical issues and is one of the best devices for producing images of soft tissues [56]. MRI machines (see Fig. 7) rely on the principle that under a strong magnetic field (often between 0.5 T and 3 T), the spin of all the protons in the human body align along the magnetic field. Radiowaves are then shown to certain areas of the body to knock the protons out

Figure 7. MAGNETOM Vida MRI scanner with a 3 T magnet and bore size of 70 cm. (Courtesy of *Siemens Healthineers*.)

of alignment. When the radiowaves stop, the protons realign to the magnetic field and emit radiowaves which are then measured. Different types of tissue can also be visualized as different tissue types take differing amounts of time to realign to the magnetic field [58]. In an MRI machine, superconductors are very often used to produce the strong magnetic fields required for in-depth images (around 70 % of MRI machines sold use superconductors). The vast majority of MRI machines use low temperature superconductors (LTS) (which is mainly because most MRI machines were invented before the discovery of HTS so a lot of designs have already been optimised for LTS and produced on a mass scale). This means that the cost of redesigning MRI machines with HTS is much greater than the potential savings from using liquid nitrogen cooling instead of liquid helium. As HTS become more commonplace it is predicted that they will become more commonly used in the manufacture of MRI machines [55].

4.2. HTS Power Cables

Another emerging technology is HTS cables in power engineering. With a global focus on reducing carbon emissions, many power transmission and distribution companies wish to minimise their carbon footprint. Currently, around 7-9 % of electrical power generated is lost over transmission and distribution networks and so companies are looking to install HTS cables as they are more efficient than regular non-superconducting cables, despite the energy usage due to refrigeration [45]. There is also the added benefit that a HTS cable of the same size as an existing conventional cable offers a two- to tenfold increase in the total power carrying capacity meaning that HTS can be retrofitted into existing conduits. For these reasons, a number of demonstration projects have been constructed to test the feasibility of HTS power cable technology.

A notable project is the Detroit Edison's HTS underground installation of an HTS cable using existing ductwork. During 1998–2003, a 120 meter demonstration cable circuit was designed and installed between the 24 kV distribution bus and a 120 kV–24 kV transformer at Detroit Edison's Frisbie substation. Impressively, the HTS cables in which copper was replaced with Ag-sheathed $Bi_2Ca_2Sr_2Cu_3O_x$ superconducting tapes

wrapped around a flexible former were able to carry triple the power compared to the existing copper cables whilst weighing 30 % of the original weight [46,47]. Although the system incorporating cables, accessories, a refrigeration system and control instrumentation was never put in operation because of leaks in the cryostat, the project significantly advanced the state of the art in the design and implementation of HTS cable systems and proved to be enlightening for subsequent efforts in this engineering field.

A similar project was undertaken by Nexans, American Superconductor (AMSC), Long Island Power Authority (LIPA) and Air Liquide Advanced Technologies on Long Island (USA) in 2007–2015 [48]. The principal objective of the project was to deploy HTS cables in a 600 meter underground segment of a 138 kV three-phase transmission circuit of the LIPA power grid. The system has been designed to operate reliably and to withstand fault currents up to 51 kA RMS. It was the first demonstration of an HTS cable at transmission voltage on the grid. Currently maintenance, cost-per-length and implementation costs are high, however, many predict that these costs will go down.

The world's first project, AmpaCity, involving installation and commissioning of the HTS superconducting cable and fault current limiter in the centre of the German city Essen was conducted by a consortium consisting of the utility company RWE, Nexans and Karlsruhe Institute of Technology [49]. The project started in 2011 and lasted for three years. The HTS cable with the fault current limiter was introduced as a connection between the medium voltage busses of two substations and replaced a conventional high voltage cable. The installed HTS cable was rated for a transmission power of 40 MVA (2310 A) at 10 kV and had a length of approximately 1 km.

The superconductor cable design for the AmpaCity project is presented in Fig.8. The three phases and common shield are arranged around the former in a concentric way, each of them separated by a lapped dielectric of polypropylene laminated paper. The three phase layers are made of stranded wires containing HTS material, all surrounded by the common braided copper shield. The cable core is placed into the cryostat consisting of two flexible corrugated tubes in concentric arrangement with vacuum insulation in between. Liquid nitrogen flows through the inlet in the former and returns through the space between the cable core and the cryostat, thus cooling the cable core to about 77 K which is well below the transition temperature of the HTS material. For medium voltage applications, the concentric arrangement of the three phases and the connection in series with a superconducting fault current limiter allows a very compact cable design which is beneficial for extremely dense urban areas.

After all required tests were successfully completed, the HTS system was finally connected to the grid in the spring of 2014. As of 2017 "the operating experience of all the cables in the world, there are more than 20 years of operating hours" [45].

The more recent German project which is currently under way is the Munich SuperLink [50], which started in 2020 and is carried out by the city utility company, Stadtwerke München, three industrial partners and two universities. It will specifically investigate how the load centre in the south of the Bavarian capital can be connected to the main feed of the transmission grid in the north by means of a 12 km long HTS cable. The target is to transmit electrical power of 500 MVA at a voltage of 110 kV using a single, slim HTS cable. Ideally, the cable will fit into partially existing empty conduits with a diameter of 150 mm, which would reduce laying costs. The superconducting wire producer, THEVA, estimated the production cost at the level of 50 euro/kAm, which currently corresponds to the performance price of copper. One can expect that the price will drop for larger scale projects which should open up new business cases.

The most recent development in the field is the announcement in 2022 by Nexans that the company has won a project to install two superconducting DC cables near Montparnasse Station in Paris [51]. This is the first time that superconducting cables will be integrated into a rail network. Two cables connecting the Vouillé substation to the overhead lines of the tracks serving Montparnasse will be commissioned in 2023. This will be a crucial step in improving the network resilience with ever growing rail traffic in megacities.

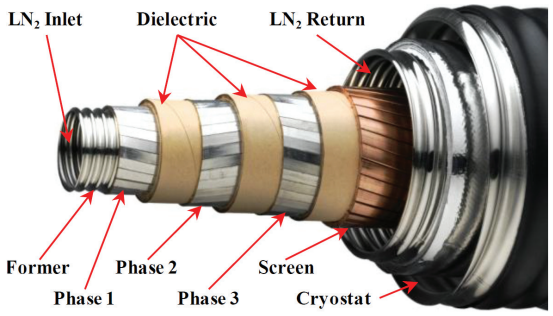

Figure 8. Three-phase power transmission cable in a concentric design. Liquid nitrogen refrigerant runs through the core of the cable to cool the superconducting tape to below the transition temperature. (Courtesy of *Nexans*.)

.

4.3. HTS Transformers

Another area of potential application is power and traction transformers used in the power transmission and distribution networks and transport. The use of superconducting wires brings about several benefits in comparison to the conventional transformers, such as higher power density, lower operating losses, lower impedance and better voltage regulations and emergency overload capability without damage to insulation or reduction of lifetime. Given the properties of HTS, it is possible to manufacture transformers with half the weight and significantly smaller footprints. This makes the transportation of transformers from the place of manufacture to the place where they are needed much easier. Finally, liquid N_2, which is used as the refrigerant for the superconductor, is more environmentally friendly in comparison to the oil normally used in transformers for cooling and dielectric purposes. This gives the added benefit of significantly reducing environmental risks associated with a leak of oil and fire.

Core losses in an HTS transformer are comparable to core losses in a similarly rated conventional transformer. Nonetheless, the overall operating losses of HTS transformers are only a small fraction of those of conventional transformers, even with the energy required to cool the superconductor to below its critical temperature. A number of demonstration projects have been successfully completed in Japan, Europe, Korea and the USA in late 1990s and early 2000s, but those efforts have ramped down and the technology has not been developed fully [52]. There is currently very little R&D being conducted on HTS transformers [45]. Research and development is still needed to reduce cryogenic and AC losses in the wires.

4.4. HTS Motors

It is predicted that HTS motors will become more and more common within everyday life. It was estimated that in 1999, 64 % of all electricity consumption in the US was due to electric motors. As seen in previous applications of superconductors, HTS motors offer increased energy efficiency (potentially reducing losses by 50 %) [53], which is desirable for both owners (who will spend less money on electricity) and governments (who aim to reduce global carbon emissions). Interestingly, HTS motors not only seem to replace existing electrical motors which are typically used in industrial settings, but due to their lower weight and smaller size are being tested for their suitability in other sectors such as transport [35].

The Naval Research Lab working on behalf of the US Navy has taken an interest in using HTS motors in ship propulsion. In July 2003, the US Navy took delivery of a 5 MW, 230 RPM ship propulsion motor from American Superconductor (see Fig. 9) in order to test proof of concept. Under a standard operating temperature of 23 K the HTS motor was able to achieve an impressive 97.7 % efficiency while also being roughly half the size and weight of a conventional motor [54]. Due to this success, a larger motor (36.5 MW) was constructed and tested, managing to achieve 97.3 % efficiency [55]. Slowly, HTS motors are being used more widely in ship propulsion systems and are set to revolutionize the industry. Encouraged by the success in naval propulsion, aircraft designs for HTS have been put forward, but as yet, no test aircraft have been made [57].

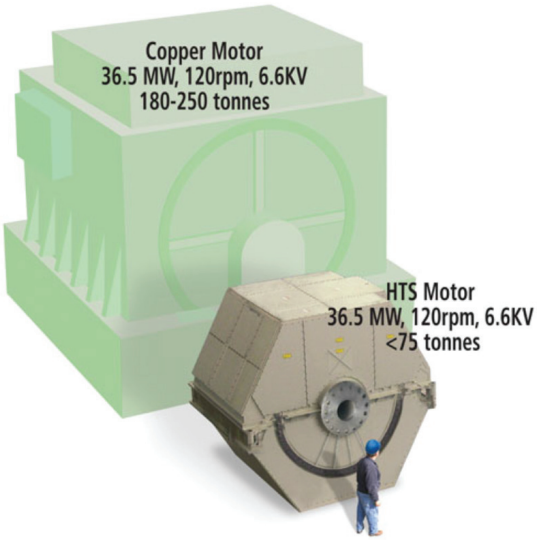

Figure 9. An illustration of the size and weight benefits of a HTS motor for ship propulsion over a traditional copper motor. From Ref. [56] with permission.

4.5. Using superconductors for energy storage

High temperature superconductivity technology also promises to produce very efficient energy storage devices. This can be achieved by either using flywheels or superconducting magnetic storage devices (SMES).

In a flywheel, a weight rapidly rotates about a fixed axis. This rapidly rotating weight stores energy in the form of kinetic energy. Energy can be added/removed from

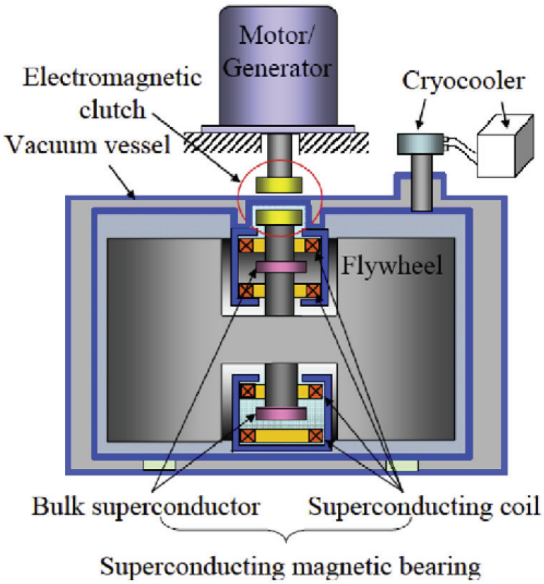

Figure 10. Construction of a flywheel with superconducting bearings. The superconductor allows the flywheel to be suspended and therefore lack any friction. From ref. [59] with permission.

.

the flywheel by the motor/generator at the top of the device. This addition/subtraction of energy from the flywheel makes the flywheel rotate faster/slower. HTS can make flywheel energy storage much more efficient by replacing traditional bearings on the shaft of the flywheel with HTS magnets which will keep the flywheel suspended, thus eliminating friction completely [58]. A number of different prototypes have been constructed which have shown the high efficiency possible compared to traditional flywheels, even with the energy needed to cool the system to below critical temperatures [58,59]. However, due to the precision engineering needed to construct a flywheel with HTS bearings, the cost of flywheels makes them more expensive than other energy storage methods [60].

HTS materials can also be used in the construction of SMES. In an SMES a DC current is allowed to flow around a closed loop. Due to the lack of resistance in this closed loop the current remains constant and hence energy can be stored. SMES have an extremely high efficiency (exceeding 90,%) even with the energy needed to power the cooling system [61]. In addition, SMES have a large power meaning that it is possible to very quickly add/ remove all the energy stored in the device. Similarly to flywheels a number of prototypes have been constructed but there has not been a widespread adoption of the technology due to the higher initial capital cost [62].

4.6. Superconductivity for fusion

With ever growing energy consumption, mankind is looking for new energy sources, with the focus being on clean energy with smaller carbon footprint; fusion is one of the most promising options for delivering this. Fusion occurs when light nuclei fuse to form a heavier nuceus and release a massive amount of energy in the process. This is the opposite of nuclear fission – the reaction that is used in nuclear power stations today – in which energy is released when a nucleus splits apart to form smaller

nuclei. Fusion is the process that takes place in the stars and provides the power that drives the universe. If nuclear fusion can be replicated on earth, it could provide virtually limitless clean, safe and affordable energy to meet the world's energy demand. Therefore, building a power plant that can harness a fusion reaction and produce electricity without generating dangerous nuclear waste associated with nuclear-fission power plants would be a very attractive idea.

Fusion occurs in the plasma state, which forms when, at extreme temperatures, gas becomes ionized meaning that electrons and their atomic nuclei separate. Plasma is usually very unstable as positively charged ions and negatively charged electrons tend to recombine. In order to force two positively charged ions get close to each other and eventually merge, the ions must have high enough kinetic energy, or, in other words, plasma must have high temperature. In addition, collisions between ions must be frequent, this sets a lower limit on plasma density. Finally, in order to maintain plasma on the Earth, where gravitational forces are much weaker as compared to those in the stars, one should be able to confine plasma by some means. For fusion to occur, the product of three parameters, plasma density, n, confinement time, τ and temperature, T, called the triple product, should exceed a specified minimum value.

To confine dense, high-energy plasma, it was proposed to use a strong magnetic field, but the field should be shaped in such a way that plasma does not touch the walls of the reactor, hence came the tokamak design. The word "tokamak" is the Russian abbreviation of TOroidal CAmera with MAgnetic Coils. The first tokamak was built in the 1960s in Kurchatov Institute in Moscow and it was then that the scientist first realised the potential of tokamaks to achieve fusion conditions. So far, the tokamak is the most heavily researched and best understood path to fusion energy [63].

For creation of strong magnetic fields, superconductivity comes into play. The first tokamak with superconducting toroidal field coils was Tokamak-7 built in Kurchatov Institute (Moscow) in the 1970s [63]. The tokamak design with superconducting coils was used later in many other implementations in different countries. The most notable ones which are still in operations are the Joint European Torus (JET), located at Culham Centre for Fusion Energy in Oxfordshire, UK; the National Spherical Torus Experiment (NSTX) at Princeton Plasma Physics Laboratory in New Jersey, USA; the Experimental Advanced Superconducting Tokamak (EAST) in Hefei, China; Korea Superconducting Tokamak Advanced Research (KSTAR) in Daejeon, South Korea and Japan Torus-60 super, advanced (JT-60SA) in Ibaraki Prefecture, Japan.

While the fusion power generated by these reactors was far below the power required to maintain fusion, important research milestones were demonstrated in the cause of the experiments that were fed into the design of more advanced machines. The main goal of all tokamak demonstrations so far is to reach breakeven fusion power, that is when the power needed to maintain fusion is equal to the power generated. Only after that a full-scale fusion power plant can be built.

The largest fusion project which is now under construction in Cadarache, France is the International Thermonuclear Experimental Reactor (ITER). The magnet system for ITER consists of four sets of large superconducting coils: 18 Toroidal Field (TF) coils, a Central Solenoid (CS), six Poloidal Field (PF) coils and 18 Correction Coils (CCs), Fig. 11 [64]. The TF coils generate the field to confine charged particles in the plasma. The CS provide the inductive flux to ramp up plasma current and contribute to plasma shaping. The PF coils provide the position equilibrium of plasma current (i.e. the fields to confine the plasma pressure) and the plasma vertical stability. The CCs allow correction of error field harmonics (up to 3 harmonics in toroidal and poloidal directions) due to, e.g., position errors. Both the TF coils and CS operate at high field

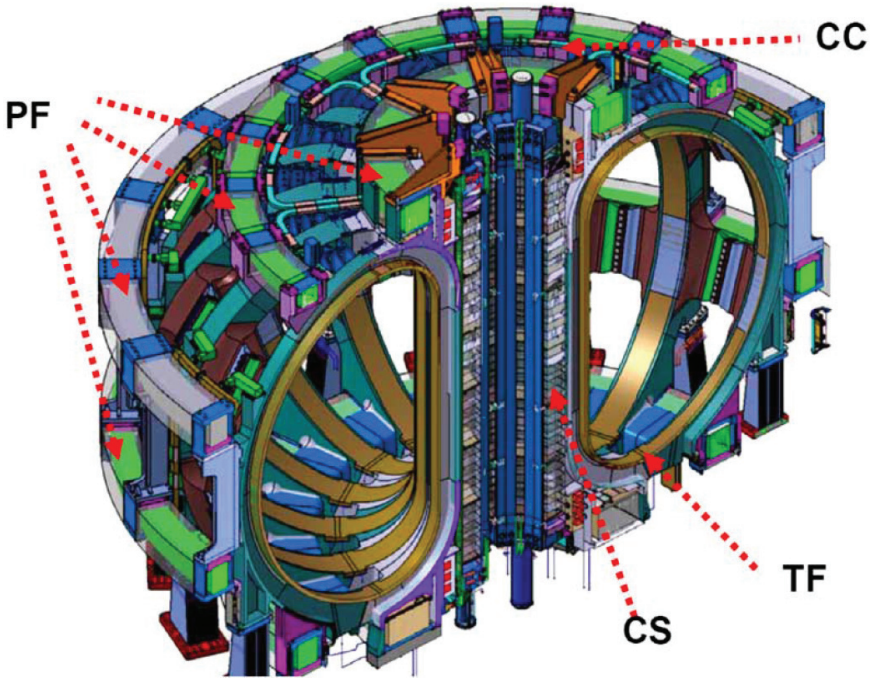

Figure 11. Superconducting coils used in the ITER. The abbreviations used are: TF - toroidal field coils; PF - poloidal field coils; CF - central solenoid and CC - correction coils. From ref. [64] with permission.

and use Nb_3Sn superconductor. The PF coils and CCs use NbTi superconductor. All coils are cooled by liquid helium to a temperature of about 4.5 K.

After the discovery of high temperature superconductors, see section 2.9, and the development HTS wire technology (section 4.2), a natural way to go would be to make magnet coils for fusion reactors using HTS materials. This would allow creation of much stronger magnetic fields. One of such projects is the ST80-HTS, a compact spherical tokamak that is being built by Tokamak Energy at the UK Atomic Energy Authority's (UKAEA's) Culham Campus, near Oxford, England. The company was founded in 2009 and adopted a new design in which a doughnut-shaped plasma is replaced by a cored apple-shaped plasma, which will help contain the plasma more efficiently [65]. The plan of Tokamak Energy is to complete building of ST80-HTS in 2026 and then design the fusion pilot plant, ST-E1. The latter is expected to produce up to 200 MW of net electrical power [66].

Another fusion project using HTS materials for coils is being conducted by Commonwealth Fusion Systems (CFS), an American company founded in 2018 [67]. They are building a SPARC tokamak that is expected to generate at least twice as much energy as is required to sustain fusion. [68]. The launch of the reactor is scheduled to take place in mid 2020s. Based on what is learned from the design and operation of SPARC, CFS plans to move as rapidly as possible to the construction of a commercial power plant.

4.7. Superconductivity for particle accelerators

Particle accelerators have a broad impact on many sectors of human activities. Progress in elementary particle science, nuclear physics and material science depend critically

on advances in accelerator science and technology.

A key component of particle accelerators is the electromagnetic resonator in the form of a cavity in which energy from the radio-frequency (RF) electric field is transferred to charged particles [69]. Typical resonance frequencies of the cavity fall in the range between 50 and 4000 MHz depending on the specific applications. The two key figures of merit of an accelerating cavity are its average accelerating electric field, E_{acc} and quality factor, Q_0. The accelerating field, also called the gradient, is the ratio of the accelerating voltage per cell, V_{c}, to the optimal cell length, $\beta\lambda/2$. Here $\beta = v/c$, where v is the particle speed and c is the speed of light in vacuum, and λ is the RF wavelength. Q_0 describes the cavity's ability to store energy: it is equal to the ratio of the total initial energy stored in the cavity to the energy dissipated per cycle, multiplied by 2π. The quality factor depends on the surface resistance, R_{s}, of the cavity material and the geometric factor, G, as $Q_0 = G/R_{\mathrm{s}}$.

Historically, RF cavities were made of copper, a conductor with extremely low R_{s}. However, this material becomes unsuitable for particle acceleration to high energies since the ohmic power loss over the cavity walls increases as the square of E_{acc}. This is especially pertinent in the continuous wave (CW) or long-pulse accelerating regimes. Here advantages of a superconducting RF (SRF) cavity come into full play. The surface resistance of a superconductor can be made many orders of magnitude smaller as compared to that of copper, resulting in the intrinsic quality factor in the $10^9 - 10^{10}$ range. SRF cavities give a net gain factor of several hundred in the overall operating power in comparison with best normal-metal cavities even after accounting for the refrigerator power.

R_{s} of superconductors can be presented as $R_{\mathrm{s}} = R_{\mathrm{BCS}} + R_{\mathrm{res}}$, where the first term is temperature dependent and the second one is temperature independent. R_{BCS} scales as $R_{\mathrm{BCS}} \propto \exp\left(-\frac{\Delta}{k_{\mathrm{B}}T}\right)$, where Δ is the energy gap of a superconductor, k_{B} is the Boltzmann's constant and T is temperature. Hence, by operating the cavity at low enough temperature, the losses associated with R_{s} can be made exponentially small in comparison to R_{res}. For niobium, an elemental superconductor with the highest critical temperature ($T_{\mathrm{c}} = 9.3\,\mathrm{K}$,) this corresponds to the working temperature of about 2 K. The remaining surface resistance R_{res} may be caused by moving flux lines and impurity heating.

Besides low ohmic losses characterised by R_{s}, another important advantage with SRF cavities is a smaller disruption of the beam. SRF systems can be shorter than those made of normal metal, and thereby the beam parameters, such as energy spread, beam halo, or the maximum current, can be significantly better. By virtue of low wall losses, SRF cavities can be designed with large beam holes (apertures) to reduce beam disruption and tolerate larger beam currents.

The development of SRF cavities for accelerators was pioneered in the early 1960s by High Energy Physics Laboratory at Stanford University. By the end of that decade they achieved a Q_0 value at low fields of 10^{11} at 1.3 K for a prototype resonator at 8.5 GHz built of solid niobium.

Superconducting cavities used in particle accelerators can be divided into two major types: those operating in the TM mode and those operating in the TEM mode. The first type is used for accelerating charged particles that move at nearly the speed of light, for example, electrons in a high-energy linear accelerator (linac) or in a storage ring. The second type is used for particles that move at a small fraction (e.g. 0.01—0.5) of the speed of light, such as heavy ions. Both types of structures could be used for particles moving at intermediate velocities.

A notable cavity example is the TESLA Test Facility (TTF) cavity is a 9-cell standing wave structure of about 1 m long whose lowest TM mode resonates at 1300 MHz. A photograph of the cavity is shown in Fig. 12. The cavity is made from 2.8 mm thick sheet high purity niobium by deep drawing of half-cells, followed by trimming and electron beam welding. This is followed by buffered chemical polishing (BCP) in order to remove a thin ($\sim 100\,\mu$m) damaged layer from the inner cavity surface to obtain good RF performance in the superconducting state. After rinsing in pure water, the cavity is annealed for 2 hours at 800°C in an ultra-high vacuum (UHV) oven, to remove dissolved hydrogen from the niobium and relieve mechanical stress in the material. This is followed by another annealing step in a different UHV oven at about 1400°C. At this temperature, all dissolved gases diffuse out of the material which improves the superconducting properties of niobium.

To operate the cavity in the superconducting state well below the critical temperature, the cavity is cooled by superfluid helium at 2 K (mind that the transition to the superfluid state occurs at 2.17 K at ambient pressure). For this, each 9-cell cavity is equipped with its own titanium liquid helium tank.

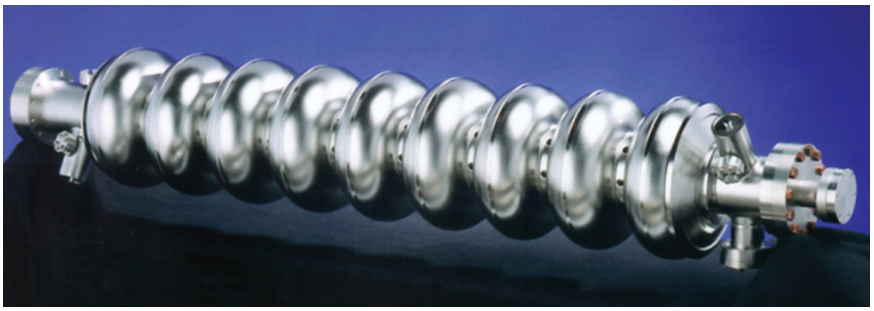

Figure 12. Superconducting 1.3 GHz 9-cell cavity for the TESLA Test Facility. From Ref. [64] with permission.

The material of choice for building SRF cavities used to be Nb for several decades, however, Nb_3Sn is gaining more attention recently as an alternative material [70]. With the transition temperature of 18 K, this superconductor offers a way to significantly increase cavity performance beyond the fundamental limits of niobium. The superconductor with higher T_c allows to reach higher E_{acc} and hence build higher energy accelerators with a lower overall length and cost. A high T_c would improve cryogenic efficiency through strong suppression of R_{BCS} for a given operating temperature and the possibility of operation at higher temperatures, where cryogenic plant efficiency is far higher than for typical niobium operating temperatures of about 2 K. Both of these factors reduce the electrical grid power requirements of a cryogenic plant, as well as the size and cost of the plant itself. In addition to these advantages for large cryogenic plants, higher temperature operation also opens the possibility of cooling a cavity with a cryocooler, thus eliminating the need for liquid helium supply. While cryogenic plants are highly efficient, they require a great deal of maintenance and operator attention. For small scale industrial accelerators, cryocoolers could greatly reduce infrastructure costs, footprint, and upkeep.

With the niobium-base SRF cavity technology mature enough, an application for building the International Linear Collider (ILC) has been put forward, to explore new physics at teraelectronvolts (trillions of electronvolts or TeV). This energy range is similar to the one used in CERN's Large Hadron Collider (LHC) in which a new type of particle, the Higgs boson, was discovered in 2012. Unlike the LHC, which is a circular

accelerator, the ILC is a 20 km-long linear particle collider that will accelerate electrons and positrons to energies around 250 GeV. To do so, it will consist of thousands of superconducting radio-frequency accelerator cavities made of niobium. The operation of the ILC would open new opportunities in physical and life sciences.

5. Electronic applications

Multiple reviews and books covering superconductive electronics are available, the most recent are the ones by A. Braginski [71] and P. Seidel [72]. Below we review applications which are rapidly developing.

5.1. Ultrasensitive SQUID-based magnetometers

Superconducting Quantum Interference Devices (SQUIDs) are the most common use of the Josephson junction [73,74]. Two versions of the SQUID have been proposed and studied in great detail: a direct current SQUID, or DC-SQUID and a radiofrequency SQUID, or RF-SQUID. The construction of a DC-SQUID is shown in Fig. 13(a). A DC-SQUID is simply a ring of superconducting material with the inclusion of two Josephson junctions in the two arms. The externally controlled parameters are the DC current I flowing through the device and magnetic flux Φ threading the SQUID loop. The voltage drop across the device V depends on both I and Φ.

For a perfectly symmetric SQUID with equal Josephson junctions, each with a critical current I_c, the predicted total critical current dependence on external magnetic flux Φ can be written as

$$I_0 = 2I_c \left| \cos\left(\frac{\pi\Phi}{\Phi_0}\right) \right| \tag{11}$$

Hence the critical current varies between its maximum value of $2I_c$ and zero. In reality, the two critical currents may be unequal, which results in a smaller variation of the total current, as shown in Fig.13(b) where the minimum current is not zero. The maximal critical current corresponds to the integer number m of fluxes threading the loop ($m = \dfrac{\Phi}{\Phi_0}$) and the minimum to half-integer.

When a SQUID is biased with a constant current $I_b > I_0$, where I_0 is the total critical current, the voltage across the device oscillates with a period of Φ_0 as a function of the external magnetic flux Φ (see Fig.13(b) and (c)). The dependence of V on Φ gives us a very accurate method of measuring magnetic flux. To measure small changes in Φ ($\ll \Phi_0$), the bias current and flux are set such that the amplitude of the voltage modulation is maximised. This corresponds to the bias current just above the critical current and the flux where the dependence $V(\Phi)$ is linear. In Fig. 13(c), this would roughly correspond to the positive slopes at $\Phi \approx 1/4\Phi_0, 5/4\Phi_0$, etc. Then by measuring voltage variations at this bias one can deduce variations of flux, and hence of external magnetic field. A typical DC SQUID at 4.2 K exhibits a flux noise of about $10^{-6}\,\Phi_0\,\mathrm{Hz}^{1/2}$ at frequencies down to about 1 Hz. Depending on the SQUID parameters, this may give a magnetic field noise as low as $1\,\mathrm{fT\,Hz}^{1/2}$.

This property is extremely useful and has found a wide variety of uses in many different areas. Examples include magnetoencephalography and magnetocardiography–the

detection of weak magnetic signals generated by brain and heart activity, correspondingly; investigation of magnetic properties of materials; biosensing in which a SQUID detects the presence of antigenes labelled with magnetic markers; microtesla NMR to investigate the structure of materials and MRI to image the human body.

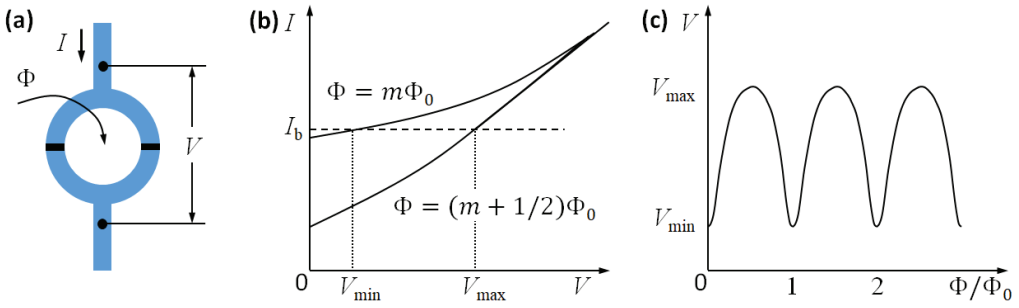

Figure 13. (a) An illustration of a SQUID. A ring is constructed out of a superconducting material. The current enters the device from the top and splits between each of the ring arms. The current then passes through each of the Josephson junctions and leaves at the bottom of the device. (b) Current-voltage characteristic of the SQUID at two values of external magnetic flux Φ_0 corresponding to the integer and half-integer numbers of Φ_0. Here m is an integer. (c) Dependence of the voltage across the device on the applied magnetic flux at a bias current I_b indicated in (b).

.

The RF-SQUID consists of a single Josephson junction integrated into a superconducting loop. It is called the RF-SQUID because its operation relies on the AC Josephson effect (see Section 2.8). Since the Josephson element is shorted at DC by the superconducting loop, the device must be monitored at high frequencies (in the range of megahertz and gigahertz). This is accomplished by coupling the device to an LC resonant circuit (usually called the tank circuit). The measured RF voltage across the tank circuit is used to read out the SQUID.

Both types of SQUIDs have been used in quantum computing experiments (see Section 5.6) either as building blocks, quantum bits, or sensitive and fast readout devices. Interestingly, applications of both types of SQUIDs are dominated by the low-T_c devices as the current technology of high-T_c SQUIDs is less mature.

5.2. Josephson voltage standard

The principle of the Josephson voltage standard is based on the AC Josephson effect described by Eq. (10), linking the voltage and frequency. This equation can be rewritten as $f_J = 2eV/h$, where $2e/h \approx 484\,\mathrm{GHz/mV}$. Hence if a finite voltage is applied to the junction, it generates AC current, whose frequency can be precisely controlled by the applied voltage. In other words, the Josephson junction is a voltage-controlled oscillator. Irradiation of the junction by external microwaves of frequency f produces constant-voltage steps on the junction's current-voltage characteristic, due to the phase locking of the Josephson oscillator by the external oscillator: $V_n = n\frac{h}{2e}f$, where an integer $n = 1, 2, ...$ denotes the step number). Clearly, the stability of voltage steps depends on frequency stability only, which can easily be in the range of 10^{-12}. This is many orders of magnitude better than the stability of Weston cells which were used as the old voltage standards.

Although the AC Josephson effect provides a much more stable voltage reference than Weston cells, the first single-junction Josephson standards were difficult to use

because they generated very small voltages, usually not more than 10 mV. In order to increase the magnitude of the reference voltage, one needs to connect many Josephson junctions in series and irradiate them uniformly with a microwave signal. This became possible due to two important technological advances. First, a reliable and reproducible fabrication process was developed, the so-called tri-layer process [75], allowing fabrication of Nb-based SIS (where S stands for a superconductor and I for an insulator) junctions on silicon substrates. Second, a clever microwave engineering solution was found such that microwave power was distributed uniformly between the junctions in the array [76]. The first practical 1 V Josephson standard was demonstrated in 1985 [77,78].

Further progress in the superconductive integrated circuit technology led to the creation of a 10 V series junction array, which typically contains between about 14,000 and 20,000 Josephson junctions depending on the details of the specific design [79,80]. They are usually arranged in several parallel arrays and operate as microstrip lines. One should bear in mind that in spite of their very successful use for DC applications, conventional Josephson voltage standards have two important drawbacks due to the ambiguity of the constant-voltage steps: they do not enable switching rapidly and reliably between different specific steps, and in addition, the constant-voltage steps are only metastable so that electromagnetic interference can cause spontaneous switching between steps.

By the end of 1980s, complete voltage metrology systems had become commercially available, and for the convenience of end-users, the commercial Josephson standards are commonly supplied with cryogenic systems. In the future, it is believed that conventional DC Josephson voltage standards will be replaced by programmable Josephson voltage standards, as these are easier to operate and may provide exciting additional possibilities and applications.

5.3. Superconducting bolometers and single-photon detectors

Generally, a bolometer is a device that absorbs certain radiation and produces an electrical signal proportional to the power of incident radiation. By improving detection sensitivity, one can reach the regime of single-photon detection, however one needs a special design for single-photon detection operation. Superconducting bolometers are used in a wide variety of fields such as: astrophysics, particle physics, material analysis and biophysics due to their ability to produce more precise measurements than existing technologies.

The most widely used types of superconducting bolometers are: superconducting tunnel junction (STJ), transition edge sensor (TES), kinetic inductance detector (KID) and hot-electron bolometer (HEB). The detection mechanisms of these devices can be summarised as follows [81]:

- The STJ [82] is based on a layered type structure consisting of a thin insulator sandwiched by two superconducting electrodes (SIS type structure). In operation as a photon detector, one of the superconducting electrodes of the STJ absorbs the photons and the energy is converted into quasiparticles (arising from broken Cooper pairs) and phonons. The STJ operates at sub-Kelvin temperatures, well below the transition temperature of the materials of constituent electrodes. Operation of the STJ relies on the detection of small current caused by tunnelling of quasiparticles from one electrode to the other. Quasiparticles are generated in the absorbing electrode due to power absorption. The STJ time constant is

typically in the range of microseconds or less (depending on the electrode area). For the operation of STJ, tunnelling of Cooper pairs must be suppressed, which is achieved by the application of an external magnetic field. STJ bolometers can detect radiation in the frequency range down to 100 GHz.

- The superconducting TES [83] utilises a very sharp resistivity change of a superconducting film around the transition temperature, hence is sensitive to small absorbed powers. The TES is usually created from a low-temperature superconducting film acting as an absorber and/or thermometer embedded in an electric circuit that generates a voltage signal upon the photon absorption. The scheme operates in the sub-Kelvin temperature range depending on the superconductor used. It can have very high photon detection efficiency and photon number resolution. TES can detect single photons from the near infrared through gamma rays as well as photon fluxes in the millimeter wavelengths range. The use of SQUID readout greatly improves detection sensitivity and allows for implementation of cryogenic multiplexing schemes in large arrays.
- The key element of a KID [84] is a superconducting microwave resonator, either in a lumped-element or distributed design. The resonance frequency and internal quality factor (Q) depend on the total resonator inductance, which has contribution from kinetic inductance. Absorption of a photon results in Cooper pair breaking (depending on the photon energy, either one or more Cooper pairs can be destroyed) which leads to quasiparticle generation. This in turn changes kinetic inductance and results in a resonance frequency shift. At the same time, the Q-factor also changes. Variation of these two parameters can be detected using a multiplexing scheme with a single feedline. KID devices exhibit optical photon detection ability; however, practical detectors in the infrared or terahertz wavelength range are still to be developed.
- The operation principle of HEB is based on the temperature dependence of the resistivity of thin disordered superconducting films in their normal state [85]. Upon absorption of a photon, a large number of quasiparticles is generated whose thermal distribution is far from thermal equilibrium. Thermalisation of such quasiparticles or "hot electrons" can occur either through the generation of phonons or by diffusion through the metallic contacts depending on the choice of superconducting material, film thickness, design and electron–phonon coupling strength. This choice determines the sensitivity and response time of the photon detector. Typical materials used for the fabrication of HEBs are Nb, NbN, Al, Ti, etc. The operation temperature for HEB detectors is usually in the mK range, and photon detection relies on the measurement of the resistance change caused by the excess of hot electrons.

With the progress of superconducting bolometer technology, it became possible to detect not only radiation power when a large flux of photons impacts on the detector, but also individual photons [86]. Such devices are called single-photon detectors and usually implemented in the nanowires, hence they were nicknamed superconducting nanowire single photon detectors, SNSPD. An SNSPD is generally comprised of a very thin and narrow superconducting strip that is cooled down well below its T_c. It is current biased at an operating value slightly below its critical current. When a photon is absorbed, superconductivity gets destroyed in a small region forming the so-called hot spot, which then expands so that a section of the strip becomes normal. As a result, an ultra-fast voltage pulse is generated. SNSPD work reliably in the infrared range of spectrum, demonstrating near-unity photon detection efficiency and outperforming

the best available semiconductor-based single photon detectors.

Besides commonly used NbN and NbTiN for operation at $T = 2...4\,\mathrm{K}$, other materials with a smaller energy gap and lower T_c are being investigated as possible candidates for operation in the terahertz and microwave frequency ranges. These include WSi or MoSi [87]. Another group of materials that is promising for bolometric applications are two dimensional superconductors, e.g., $NbSe_2$. The smaller heat capacity of $NbSe_2$ flakes holds the promise of drastically improving the sensitivity of bolometers.

Superconducting bolometers have already found applications in radioastronomy and are being successfully used in spaceborne missions and numerous ground-based and airborne observations. Their single-photon detection capability in various frequency ranges can be invaluable for quantum computing and quantum communication as well as in search for dark matter.

5.4. Superconducting parametric amplifiers

The operation principle of a parametric amplifier is based on the modulation of a reactive parameter, a capacitance or inductance, of an electric circuit by an external signal, the pump. In this case energy gets transferred from the pump frequency mode, ω_p, to the signal frequency mode, ω_i, via the creation of the third mode, ω_i, called the idler. Parametric amplification can occur either via a four-wave or three-wave mixing processes, often referred to as the four-photon and three-photon regimes, for which the relation between the signal, idler and pump angular frequencies are $\omega_s + \omega_i = 2\omega_p$ and $\omega_s + \omega_i = \omega_p$, respectively. The early implementations of parametric amplifiers were based on the varactor, a semiconductor component whose capacitance can be controlled by an external voltage [88].

One of the advantages of parametric amplifiers is that gain is produced without dissipating heat in the reactive component, therefore, the noise added by the amplifier (referred to its input) can approach the minimum allowed by quantum mechanics, $T_N = \hbar\omega/2k_B$ (or $24\,\mathrm{mK/GHz}$), for a phase-preserving amplifier, that is, one that equally amplifies both quadratures. Here T_N is the noise temperature, ω is the amplifier's operating frequency.

With the discovery of the Josephson effect and invention of the Josephson tunnel junction in the early 1960s (see sub-section 2.8), it was realised that this element is an ideal component for building parametric amplifiers due to its non-linear inductance and zero dissipation (see review [89]). The current-dependent Josephson inductance can be written as

$$L_J = \frac{L_{J0}}{\sqrt{(1 - I/I_c)^2}}, \tag{12}$$

where L_{J0} is the Josephson inductance at zero bias current.

Since the first realization of the Josephson parametric amplifier (JPA) in the late 1960s, enormous progress has been made in the development of JPAs. In recent years, superconducting parametric amplifier devices have seen renewed interest. The greatest motivation driving this development is the necessity for detecting extremely weak signals when reading out quantum circuits or searching for dark matter.

Besides using single Josephson junctions as non-linear inductances, one can also use double junctions in the SQUID geometry (see sub-section 5.1) whose inductance

depends also on the external magnetic flux:

$$L_{\mathrm{SQUID}} = \frac{L_J(I)}{2\cos\pi\Phi/\Phi_0}, \tag{13}$$

which allows the use of magnetic flux as a pump signal.

One of the drawbacks of JPAs is the relatively narrow bandwidth which is determined by the quality factor of the resonator. To get around this issue, one can use the so-called travelling wave regime, which is completely analogous to the propagation of optical signal in a non-linear medium [90]. For this, an artificial one-dimensional medium is constructed in the form of an array of identical Josephson junctions or SQUIDs, playing the roles of atoms, through which both the pump and signal microwave tones can propagate. Such amplifiers are called Josephson travelling wave parametric amplifiers (JTWPAs).

In parallel to the development of JTWPAs, an alternative approach to building travelling wave amplifiers has also been developed. It is based on using non-linear kinetic inductance of highly disordered superconducting thin films made of, for example, TiN of NbTiN (KITWPAs). The kinetic inductance of such films can written as

$$L_{\mathrm{k}}(I) \approx L_{\mathrm{k}}(0)[1 + (I/I_*)^2] \tag{14}$$

for $I \ll I_*$, where I_* sets the scale of non-linearity and is comparable to I_c. The zero-current kinetic inductance $L_{\mathrm{k}}(0)$ depends on the normal-state resistance of the film R_n (the resistance just before the superconducting transition) and superconducting energy gap Δ as $L_{\mathrm{k}}(0) = \hbar R_n/\pi\Delta$.

Travelling wave parametric amplifiers are more challenging to implement in comparison to their resonator-based counterparts. First, construction of a long non-linear medium requires more advanced nanofabrication methods with a better control of the device parameters. Second, the impedance of the amplifier must be $50\,\Omega$-matched to the external microwave circuit. Third, phase matching conditions must be satisfied for the signal, pump and idler tones. Despite all these challenges, several successful experiments have been performed demonstrating JTWPAs and KITWPAs with gain of 10–20 and bandwidth of several GHz [90].

5.5. Digital SFQ circuits

The proposal to make a digital computer (a computer with two logic levels) using superconductors instead of semiconductors was first conceptualized in 1956 by Buck [91]. In his superconductor-based computer, all logic gates are constructed with a cryotron circuit element instead of a traditional semiconductor transistor. A cryotron is a technically simple device and has two components: a superconducting wire and a superconducting control winding. The superconducting control winding is made from a superconductor with a higher T_c and it is covered in an insulator. The control winding is wrapped around the superconducting wire. When a current is applied to the control winding, a magnetic field is generated around the winding quenches the superconductivity in the wire making the wire resistive. The ability of the control winding to control the state of the wire (its resistance is either zero or finite) produces the logic element. This idea promised a very low power dissipation, but it was limited by the fact that switching speed was lower than existing semiconductor switches.

After the invention of the Josephson junction, another superconducting cryotron concept was proposed. In 1967 J Matisoo (working in the IBM's Thomas J. Watson Research Center) published his concept for the tunnelling cryotron [92]. In this device, a Josephson junction is created by overlapping two superconductors and using the oxide layer on the superconductor as the insulator. As discussed previously, Josephson junctions have a critical current. With the addition of a control above the junction, the resistance of the junction can be controlled by applying a current to the control. The benefit of this type of cryotron is that there is no superconducting to resistive transition that was previously present, meaning that the switching time can be significantly shorter (less than 1 ns). This device was based on latching logic and pursued in the USA and Japan, however, this approach was abandoned as not being competitive enough with rapidly developing semiconductor electronics.

In the mid 1980s, the group headed by Konstantin Likharev at Moscow State University in the USSR had come up with an entirely new idea: to use the single magnetic flux quantum Φ_0 to represent logical states. This concept became known as the Rapid Single Flux Quantum (RSFQ) logic [93,94]. The basic cell of the scheme is a SQUID loop with its two binary states represented by the presence or absence of Φ_0 in the loop. Switching between the two states generates a short voltage pulse which can propagate to another cell and thus pass information. While the energy dissipation per bit of operation in such circuits was extremely small, $\approx 10^{-18}$ J/bit, the overall dissipation was dominated by an order of magnitude larger dissipation in the resistive current biasing network of each cell. To mitigate this problem, the whole on-chip DC current biasing network was replaced by inductors and current-limiting Josephson junctions [95]. This approach required the use of high-inductance bias lines which was made possible by introducing an extra superconducting layer with high kinetic inductance.

Over the past three decades, fabrication of superconducting integrated circuits (ICs) have become a mature technology, with superconducting foundries existing in the USA and Japan [96,97]. Nb-based multilayer integrated circuits containing tens of thousands Josephson junctions can be fabricated with small parameter variation for operation at about 4 K. Superconducting digital ICs outperform their semiconductor counterparts by at least a factor of 10 in terms of energy dissipation per bit of operation, even including the energy required for cryocooling. Another advantage of superconducting digital ICs is that their clock frequency can be maintained in the range of tens or even hundreds of GHz while the present-day semiconductor technology which runs at around 4 GHz. Nonetheless, the superconducting computer has not become a reality yet and whether or not it will become depends on further progress in the field. The major drawback of superconductor ICs is their relatively small density of integration. For example, modern semiconductor chips contain $\sim 10^9$ transistors per cm^2, while the density of Josephson junctions is almost four orders of magnitude lower. In order to become competitive with semiconductor electronics, superconducting circuits must reach a much higher integration density to have the circuit complexities required for computing. This is a very challenging task given the dimensions of SQUID loops and all auxiliary elements such is bias inductors and shun resistors.

Despite all these difficulties, RSFQ technology and its variations based on manipulation of individual magnetic flux quanta provides a viable route to some useful applications where low temperature environment is a must. For example, superconducting digital circuits can be used as control electronics for very large arrays of cryogenic bolometers (see Section 5.3); adiabatic and gate-based quantum computing architectures based on superconducting qubits and operating at millikelvin temperatures (see Section 5.6) and also as cryogenic data processors when reading out a large number

of cryogenic sensors. Bringing control and readout electronics closer to quantum circuits operating at much lower temperatures requires modifications in the fabrication recipe of the former, but this technical task has already been carried out and the superconducting Josephson junction fabrication process tailored for lower temperature integrated digital circuits has been implemented, optimized and fully tested [97].

5.6. Quantum computers

To discuss quantum computing, a brief insight into quantum mechanics is given. Firstly, we can think of an electron being stuck in a small, arbitrarily defined box surrounded by nothing. The electron in this box can be described by a variable quantity called a wavefunction which should satisfy the Schrödinger equation with certain boundary conditions [98]. Because the electron is stuck in the box, there are a set number of solutions to this equation as the wavefunction of the electron must be zero at the walls of the box. As a result, the electron can only occupy particular quantum states corresponding to discrete energy levels, this is called energy level quantisation. Quantum states are usually denoted as $|0\rangle$, $|1\rangle$, etc. One of the most intriguing properties of quantum objects is that they can occupy more than one state at the same time (often called a superposition of states). If only two basis states are used, an object called a quantum bit (also referred to as a qubit) can be created. This means that information can be encoded not only using 0 and 1 states, as done in conventional computers, but also any desired superposition of the two states. Hence the state of a qubit described by the wavefunction ψ can be presented as $\psi = \alpha|0\rangle + \beta|1\rangle$, where α and β are complex amplitudes satisfying the normalisation condition $|\alpha|^2 + |\beta|^2 = 1$. This way the qubit may take any state out of the continuum of available states. The ability of the system to remain in a superposed state (involving two or more basis states) is called quantum coherence. The idea in quantum computing is to use processors comprising a large number of qubits for processing information using quantum algorithms [99]. This means that the computational power of quantum computers exponentially increases with the addition of each qubit compared to conventional digital computers. However, quantum coherence is often difficult to achieve as superposition is lost when the wavefunction collapses and the electron is found to be in a certain state with a certain energy. Therefore a key challenge of constructing a quantum computer is reducing the electron's interaction with the outside world (decoupling it from its environment) and thus ensuring that it remains in the quantum regime so that it can stay in two states simultaneously.

Since the advent of quantum mechanics, it was commonly believed that only microscopic objects such as atoms or electrons can possess quantum properties such as superposition of quantum states. However, at the end of the last century it was demonstrated that quantum coherent dynamics was possible in superconductors. A so-called 'Cooper pair box' made from aluminium (which becomes superconducting below about 1.2 K) was constructed containing around 10^8 Cooper pairs and the states with N and $N + 1$ Cooper pairs could be distinguished due to the so-called Coulomb blockade effect. By applying fast voltage pulses to the device it was possible to prepare the system in different superpositions (in other words, control coefficients α and β) and measure such states using a special probe. This experiment is now regarded as the first demonstration of the solid-state qubit [100]. Later, other types of superconducting qubits with better coherent properties have been constructed, based on different degrees of freedom. It is not surprising that superconducting qubits outperform other types of

solid-state qubits: superconductors can carry electric current with zero dissipation, which is a good prerequisite for quantum coherence. Also, they have a well-defined energy level, which is separated from the other levels by the energy gap, protecting fragile quantum states from decoherence. An important property of superconducting qubits is that they allow scaling up of digital circuits. This means that it is possible to add a larger number of qubits (meaning that more complicated calculations can be performed) while the qubits still remain coherent [101].

These days quantum computing with superconducting circuits has become an area of active research attracting not only academia, but also a large number of industrial players including such giants as Google, IBM and Raytheon to mention a few. Besides superconductors, other types of solid-state and non-solid-state technologies are being actively pursued, however, it is still not clear what approach will be the winner in this race.

6. Conclusions

In this review, we have given a brief history of the discovery and development of the field of superconductivity, concentrating on the main discoveries within the field. Given the complexity of the phenomena, we have not been able to mention all the theories proposed or the discoveries made. In addition, we have listed some of the present applications of superconductors, but this is not comprehensive as it is a rapidly progressing field with many other developments predicted in the future. One example of this, MAGLEV (MAGnetic LEVination) trains are able to travel at extremely high speeds (the world record is 581 km/h) compared to existing high-speed trains which travel between 300 and 320 km/h [102,103]. According to the Chinese TV network CGTN, China has successfully completed the country's first full-size superconducting test run for an ultra-high-speed MAGLEV train, and is set to test a 1,000 km/h ultra-high-speed train [104].

The European Commission recognised the potential for the use of superconducting cables in the future electricity grid in 2022 by funding a large project called SCARLET which has the goal of bringing the technology to the brink of commerialisation [105]. The project involving several industrial and academic partners will, over a period of 4.5 years, bring this new power cable technology to commercial performance levels. This will allow the electric power transmission and distribution companies to use cables that can transfer very high power over very small conductors, thus improving efficiency as well as environmental impact and footprint.

In aviation, the goal of the current ASCEND demonstrator project by Airbus UpNext is to produce a major breakthrough in electric propulsion for long range aircraft by utilising an electric or hybrid electric propulsion system based on cryogenic and superconducting technologies. This may be more than 2 to 3 times lighter than a conventional system and would significantly boost the perform of electric and hybrid electric propulsion systems in future low emission aircraft [106].

The holy grail of the field – a material that exhibits superconductivity at room temperature – is still an unrealised possibility which, if found, has the potential to revolutionise the world. Room temperatures superconductors would offer enormous advantages over current technologies with dramatic drops in power consumption and increases in device performances, as device sensitivity is often limited by Nyquist noise (which is proportional to resistance). However, even in the absence of room temperature superconductors for the present, existing cryogenic superconductors continue to

offer a wide number of benefits across many different sectors. This is why superconductivity will continue to play an important and increasing role in the world around us and will be explored with interest by scientists and engineers for many years to come.

Acknowledgement

Proof-reading of the manuscript by B. Mercer is gratefully acknowledged.

Funding

YAP acknowledges partial support from the QSHS project ST/T006102/1 funded by STFC.

Notes on contributors

The manuscript was drafted by WJM under the guidance of YAP. The final version was completed by YAP.

References

[1] Encyclopedia Britannica: superconductivity. [cited 2023 Jun 19]. Available from: https://www.britannica.com/science/superconductivity

[2] Blundell S Superconductivity. A very short introduction. New York (NY): Oxford University Press; 2009.

[3] Kamerlingh Onnes H. 1911. Communications from the Physical Laboratory at the University of Leiden, No 124g.

[4] Van Delft D, Kes P. The discovery of superconductivity. Phys Today 2010;63:38–43.

[5] Physics World, April 2011.

[6] Rogalla H, Kes PH, editors. 100 Years of superconductivity. Boca Raton (FL): CRC Press; 2012.

[7] Wilson MN. 100 years of superconductivity and 50 years of superconducting magnets. IEEE Trans Appl Supercond. 2012;22:3800212.

[8] Kamerlingh Onnes H. 1913. Communications from the Physical Laboratory at the University of Leiden, Suppl. 34.

[9] Kamerlingh Onnes H. 1914. Communications from the Physical Laboratory at the University of Leiden, No 139f.

[10] Huebener RP, Lübbig H. A focus of discoveries. Singapore: World Scientific; 2012.

[11] Meissner W, Ochsenfeld R. Ein neuer Effekt bei Eintritt der Supraleitfähigkeit. Naturwissenschaften 1933;21:787–788.
Translated by Forrest AM. Eur. J. Phys. 1983;4:117–120.

[12] London F, London H. The electromagnetic equations of the supraconductor. Proc Royal Soc. Series A-Mathematical and Physical Sciences, 1935;149(866):71–88.

[13] Seeber B. editor, Handbook of applied superconductivity. Boca Raton: CRC Press; 1998. (vol 2).

[14] de Haas W, van Aubel E, Voogd J. A superconductor consisting of two nonsuperconductors. Akademie der Wetenschappen, Amsterdam, Proceedings, 1929;32:730.

[15] Casimir-Jonker, JM, De Haas WJ. Some experiments on a supraconductive alloy in a magnetic field. Physica 1935;2(1-12):935–942.
[16] Rjabinin JN, Schubnikow L. Über die Abhängigkeit der magnetischen Induktion des supraleitenden Blei vom Feld. Physikalischer Zeitschrift der Sowjet Union, 1935;6:557–568.
[17] Mendelssohn K, Moore JR. Supra-conducting alloys. Nature 1935;135(3420):826–827.
[18] Mendelssohn K, Moore JR. Specific heat of a supraconducting alloy. Proc. Royal Soc. Series A-Mathematical and Physical Sciences. 1935;151(873):334–341.
[19] Shubnikov LV, Khotkevich VI, Shapelev YuD. et al. Zh Eksp Teor Fiz. 1937;7:2.
[20] Ginzburg VL, Landau LD. To the theory of superconductivity. Zh Eksp Tear Fiz., 1950;20:1064–1082.
[21] Tinkham M. Introduction to superconductivity. New York (NY) Dover Publications. 2004 pp.12.
[22] Cyrot M. Ginzburg-Landau theory for superconductors. Rep Prog Phys. 1973;36(2):103–158.
[23] Reynolds CA, Serin B, Wright WH, et al. Superconductivity of isotopes of mercury. Phys Rev. 1950;78(4):487.
[24] Maxwell E. Isotope effect in the superconductivity of mercury. Phys Rev. 1950;78(4):477.
[25] Fröhlich H. Theory of the superconducting state. I. The ground state at the absolute zero of temperature. Phys Rev. 1950;79(5):845–856.
[26] Cooper LN. Bound electron pairs in a degenerate Fermi gas. Phys Rev. 1956;104(4):1189–1190.
[27] Bardeen J, Cooper LN, Schrieffer JR. Theory of superconductivity. Phys Rev. 1957;108:1175–1204.
[28] Simon SH. The Oxford Solid State Basics. Oxford University Press: 2013.
[29] Abrikosov AA. On the magnetic properties of superconductors of the second group. Sov Phys. 1957;32:1174–1182.
[30] Abrikosov AA. Nobel Lecture: Type-II superconductors and the vortex lattice. Rev Mod Phys. 2004;76(3):975–979.
[31] Gor'kov LP. Microscopic derivation of the Ginzburg-Landau equations in the theory of superconductivity. Sov Phys JETP, 1959;9(6):1364–1367.
[32] Josephson BD. 1962. Possible new effects in superconductive tunnelling. Phys Lett, 1962;1(7):251–253.
[33] Anderson PW, Rowell JM. Probable observation of the Josephson superconducting tunneling effect. Phys Rev Lett. 1963;10(6):230–232.
[34] Beasley MR, Geballe TH. Superconducting materials. Phys Today, 1984;37(10):60–68.
[35] Plakida N. High-temperature cuprate superconductors: Experiment, theory, and applications (Vol. 166). Berlin: Springer; 2010.
[36] Müller KA, Bednorz JG. High-temperature superconductivity. PNAS, 1987;84(14):4678–4680.
[37] Hock KH, Nickisch H, Thomas H. Jahn-Teller effect in itinerant electron-systems-the Jahn-Teller polaron. Helvetica Phys. Acta, 1983;56(1-3):237–243.
[38] Bednorz JG. and Müller KA. Possible highT_c superconductivity in the Ba-La-Cu-O system. Z Phys B Condensed Matter 1986;64:189–193.
[39] Wu MK, Ashburn JR, Torng C et al. Superconductivity at 93 K in a new mixed-phase Y-Ba-Cu-O compound system at ambient pressure. Phys Rev Lett. 1987;58(9):908–910.
[40] Bussmann-Holder A, Keller H. High-temperature superconductors: underlying physics and applications. Z. Naturforsch. 2020;75(1–2)b:3–14.
[41] Nagamatsu J, Nakagawa N, Muranaka T et al. Superconductivity at 39 K in magnesium diboride. Nature 2001;410:63–64.
[42] Kamihara Y, Hiramatsu H, Hirano M et al. Iron-based layered superconductor: LaOFeP. J Am Chem Soc. 2006;128(31):10012–10013.
[43] Yntema G. Niobium superconducting magnets. IEEE Trans Magn. 1987;23(2),390–395.
[44] Davies FJ. MRI magnets. In: Weinstock H, editor. Applications of Superconductivity.

Dordrecht (The Netherlands): Kluwer Academic Publishers; 2000. p.385–414.
[45] Marchionini BG, Yamada Y, Martini L, Ohsaki H. High-temperature superconductivity: a roadmap for electric power sector applications, 2015–2030. IEEE Trans Appl Supercond. 2017;27(4):1–7.
[46] Steve N, Nassi M, Bechis M et al. High temperature superconducting cable field demonstration at Detroit Edison. Physica C: Superconductivity, 2001;354(1-4):49–54.
[47] Kelley N, Wakefield C, Nassi M et al. HTS cable system demonstration at Detroit Edison. Proceedings of the 2001 IEEE/PES Transmission and Distribution Conference and Exposition. Developing New Perspectives; 2001 November 2; Atlanta (GA): IEEE Xplore; 2002.
[48] Final Technical Report, HTS Transmission Cable System for Installation in the Long Island Power Grid. AMSC; October 5, 2015.(DOE Award DE-FC26-07NT43240).
[49] Stemmle M, Merschel F, Noe M et al. Ampacity project – Worldwide first superconducting cable and fault current limiter installation in a German city center. Proceedings of the 22nd International Conference and Exhibition on Electricity Distribution (CIRED 2013); 2013 June 10–13; Stockholm: IEEE Xplore; 2013.
[50] Transformers Magazine. Special Edition: Superconductivity. 2021.
[51] A world-first in France at Montparnasse train station: Nexans installs superconducting cables to strengthen and secure the power supply [Internet]. 2022 Jun 9; [about 4 screens]. Available from: https://www.nexans.com/en/newsroom/news/details/2022/06/a-world-first-in-France-at-montparnasse-train-station-nexans-installs-superconducting-cables.html
[52] Jin J, Chen X. Development of HTS Transformers. 2008 IEEE International Conference on Industrial Technology, Chengdu, 2008, pp. 1-6, doi: 10.1109/ICIT.2008.4608455.
[53] Morrison G. Superconductors power up. Mech Eng. 1999;121(01):46–50.
[54] Snitchler G, Gamble B, Kalsi SS. The performance of a 5 MW high temperature superconductor ship propulsion motor. IEEE Trans Appl Supercond. 2005;15(2):2206–2209.
[55] Gamble B, Snitchler G, MacDonald T. Full power test of a 36.5 MW HTS propulsion motor. IEEE Trans Appl Supercond. 2010;21(3):1083–1088.
[56] La Rosa Betancourt M, Ballester BM, O'Regan R et al. UDT 2019–Technology trends and challenges for superconductor-based ship propulsion. Proceedings of the 32nd Undersea Defence Technology Conference; 2019 May 13–15; Stockholm, Sweden.
[57] Yazdani-Asrami M, Zhang M, Yuan W. Challenges for developing high temperature superconducting ring magnets for rotating electric machine applications in future electric aircrafts. J Mag Magn Mater. 2021;522:167543.
[58] Boyes JD, Clark NH. Technologies for energy storage. Flywheels and superconducting magnetic energy storage. In 2000 Power Engineering Society Summer Meeting (Cat. No.00CH37134) (Vol. 3, pp. 1548-1550). 2000, July.
[59] Nagashima K, Seino H, Sakai N et al. Superconducting magnetic bearing for a flywheel energy storage system using superconducting coils and bulk superconductors. Physica C 2009;469(15-20):1244–1249.
[60] Hall PJ, Bain EJ. Energy-storage technologies and electricity generation. Energy Policy, 2008;36(12):4352–4355.
[61] Buckles W, Hassenzahl WV. Superconducting magnetic energy storage. IEEE Power Eng Rev. 2000;20(5):16–20.
[62] Yuan W, Xian W, Ainslie M et al. Design and test of a superconducting magnetic energy storage (SMES) coil. IEEE Trans Appl Supercond. 2010;20(3):1379–1382.
[63] Mitchell N et al. Superconductors for fusion: a roadmap. Supercond Sci Technol. 2021;34:103001.
[64] Mitchell N, Bessette D, Gallix R et al. The ITER Magnet System. IEEE Trans Appl Supercond. 2008;18(2):435–440.
[65] Sykes A, Costley AE, Windsor CG et al. Compact fusion energy based on the spherical tokamak. Nucl Fusion 2018;58:016059.
[66] Tokamak Energy Ltd [Internet]. [cited 2023 Jun 19]. Available from:

https://www.tokamakenergy.co.uk/technology/
[67] Commonwealth Fusion Systems [Internet]. [cited 2023 Jun 19]. Available from: https://cfs.energy/
[68] Creely AJ, Greenwald MJ, Ballinger SB et al. Overview of the SPARC tokamak. J Plasma Phys. (2020);86:865860502.
[69] Padamsee H. 50 years of success for SRF accelerators–a review. Supercond Sci Technol. 2017;30:053003.
[70] Posen S, Hall DL. Nb_3Sn superconducting radiofrequency cavities: fabrication, results, properties, and prospects. Supercond Sci Technol. 2017;30:033004.
[71] Braginski AI. Superconductor electronics: Status and outlook. J Supercond Nov Magn. 2019;32:23–44.
[72] Seidel P, editor. Applied Superconductivity: Handbook on devices and applications. Vol. 2. Weinheim: 2015; Wiley; 2015.
[73] Clarke J, Braginski AI, editors. The SQUID Handbook. Vol. I. Weinheim: Wiley; 2004.
[74] Clarke J, Braginski AI, editors. The SQUID Handbook. Vol. II. Weinheim: Wiley; 2006.
[75] Gurvitch M, Washington MA, Huggins HA. High quality refractory Josephson tunnel junctions utilizing thin aluminum layers. Appl Phys Lett. 1983;42(5):472–474.
[76] Niemeyer J, Hinken, JH, Kautz RL. Near-zero bias arrays of Josephson tunnel junctions providing standard voltages up to 1 V. IEEE Trans Instrum Meas. 1985;IM-34(2):185–187.
[77] Hamilton CA, Kautz RL, Steiner RL et al. A practical Josephson voltage standard at 1 V. IEEE Electron Device Lett. 1985;6(12):623–625.
[78] Niemeyer J, Grimm L, Meier W et al. Stable Josephson reference voltages between 0.1 and 1.3 V for high-precision voltage standards. Appl Phys Lett. 1985;47(11):1222—1223.
[79] Hamilton CA, Lloyd FL, Chieh K et al. A 10-V Josephson voltage standard. IEEE Trans Instrum Meas. 1989;38(2):314–316.
[80] Pöpel R, Niemeyer J, Fromknecht R et al. 1- and 10-V series array Josephson voltage standards in Nb/Al2O3/Nb technology. J Appl Phys. 1990;68(8):4294–4303.
[81] Morozov DV, Casaburi A and Hadfield RH, Superconducting photon detectors. Contemp Phys. 2021;62:69–91.
[82] A. Peacock et al. Single optical photon detection with a superconducting tunnel junction. Nature 1996;381:135-–137.
[83] Andrews DH, Brucksch WF, Jr., Ziegler WT et al. Attenuated superconductors I. For measuring infra-red radiation. Rev Sci Instrum. 1942;13:281–292.
[84] Day PK, LeDuc HG, Mazin BA et al. A broadband superconducting detector suitable for use in large arrays. Nature, 2003;425:817–821.
[85] Shurakov A, Lobanov Y, Goltsman G. Superconducting hot-electron bolometer: from the discovery of hot-electron phenomena to practical applications. Supercond Sci Technol. 2016;29:023001.
[86] Gol'tsman GN et al. Picosecond superconducting single-photon optical detector. Appl Phys Lett. 2001;79:705–707.
[87] Natarajan CN, Tanner MG, Hadfield RH. Superconducting nanowire single-photon detectors: physics and applications. Supercond Sci Technol. 2012;25:063001.
[88] Penfield P, Rafuse RP. Varactor Applications. Cambridge (MA): MIT Press, 1962.
[89] Aumentado J. Superconducting parametric amplifiers. IEEE Microw Mag. 2020;21(8):45–59.
[90] Esposito M, Ranadive A, Planat L et al. Perspective on traveling wave microwave parametric amplifiers. Appl Phys Lett. 2021;119:120501.
[91] Buck DA. The cryotron - a superconductive computer component. Proc IRE. 1956;44(4):482–493.
[92] Matisoo J. The tunneling cryotron - A superconductive logic element based on electron tunneling. Proc IEEE. 1967;55(2):172–180.
[93] Likharev KK, Mukhanov OA, Semenov VK. Resistive single flux quantum logic for the Josephson junction technology. In: Hahlbohm HD, Lübbig H, editors. SQUID '85: Superconducting quantum interference devices and their applications. Berlin: W. de Gruyter

Publishers; 1985. p. 1103–1108.
[94] Likharev KK, Semenov VK. RSFQ logic/memory family: a new Josephson-junction technology for sub-terahertz-clock-frequency digital systems. IEEE Trans Appl Supercond. 1991;1:3–28.
[95] Mukhanov O. Energy-efficient single flux quantum technology. IEEE Trans Appl Supercond. 2011;21(3):760–769.
[96] Tolpygo SK. Superconductor digital electronics: Scalability and energy efficiency issues. Low Temp Phys. 2016;42(5):361–379.
[97] Yohannes D, Renzullo M, Vivalda J et al. High density fabrication process for single flux quantum circuits. Appl Phys Lett. 2023;122:212601.
[98] Griffiths DJ, Schroeter DF. Introduction to quantum mechanics. 3rd ed. Cambridge (UK): Cambridge University Press; 2018.
[99] Nielsen MA, Chuang IL. Quantum computation and quantum information. 10th anniversary ed. Cambridge (UK): Cambridge University Press; 2010.
[100] Nakamura Y, Pashkin YA, Tsai JS. Coherent control of macroscopic quantum states in a single-Cooper-pair box. Nature 1999;398:786–788.
[101] Ripoll JJG. Quantum information and quantum optics with superconducting circuits. Cambridge (UK): Cambridge University Press; 2022.
[102] Lee HW, Kim KC, Lee J. Review of maglev train technologies. IEEE Trans Magn. 2006;42:1917–1925.
[103] Han HS, Kim DS. Magnetic levitation: Maglev technology and applications. Dordrecht: Springer Science+Business Media; 2016. (Roess RP, editor. Springer tracts on Transportation and Traffic; vol.13).
[104] China set to test 1,000 km/h ultra-high-speed maglev train [Internet]. 2023 Apr 24 [cited 2023 Jun 18] Available from: https://news.cgtn.com/news/2023-04-24/China-set-to-test-1-000km-h-ultra-high-speed-maglev-train-1jgCFqBvmq4/index.html
[105] Superconducting cables for Europe's clean energy future; 2022 Oct 10 [cited 2023 Jun 19]. Available from: https://www.rifs-potsdam.de/en/news/superconducting-cables-europes-clean-energy-future
[106] Ybanez L, Colle A, Nilsson E. et al. ASCEND: The first step towards cryogenic electric propulsion. IOP Conf Ser.: Mater Sci Eng. 2022;1241:012034.